

# Large deviation theory-based adaptive importance sampling for rare events in high dimensions\*

Shanyin Tong<sup>†</sup> and Georg Stadler<sup>‡</sup>

**Abstract.** We propose a method for the accurate estimation of rare event or failure probabilities for expensive-to-evaluate numerical models in high dimensions. The proposed approach combines ideas from large deviation theory and adaptive importance sampling. The importance sampler uses a cross-entropy method to find an optimal Gaussian biasing distribution, and reuses all samples made throughout the process for both, the target probability estimation and for updating the biasing distributions. Large deviation theory is used to find a good initial biasing distribution through the solution of an optimization problem. Additionally, it is used to identify a low-dimensional subspace that is most informative of the rare event probability. This subspace is used for the cross-entropy method, which is known to lose efficiency in higher dimensions. The proposed method does not require smoothing of indicator functions nor does it involve numerical tuning parameters. We compare the method with a state-of-the-art cross-entropy-based importance sampling scheme using three examples: a high-dimensional failure probability estimation benchmark, a problem governed by a diffusion equation, and a tsunami problem governed by the time-dependent shallow water system in one spatial dimension.

**Key words.** Rare events, large deviation theory, adaptive importance sampling, cross-entropy method, likelihood-informed subspace, reliability analysis.

**AMS subject classifications.** 65C05, 60F10, 62L12, 65F15, 65K10

**1. Introduction.** Accurate probability estimation of rare, high-impact events in complex systems with uncertainties is important in many areas. Examples of such events include the structural failure of engineered systems, geophysical disasters, extreme weather patterns, global disease outbreaks, and the collapse of markets or financial systems. Estimating the probability that such events occur is crucial, e.g., for hazard preparedness, for insurances companies, and generally to make decisions about how to mitigate the effects of such events.

To formulate the rare event probability estimation problem mathematically, we consider the probability space  $(\Omega, \mathcal{B}(\Omega), \mathbb{P})$  with a probability measure  $\mathbb{P}$ . The uncertain parameter  $\boldsymbol{\theta}$  is modeled as a random vector on  $\Omega$  as  $\boldsymbol{\theta} : \Omega \rightarrow \Theta \subseteq \mathbb{R}^n$  with  $\Theta$  is a measurable set. We assume that the distribution of  $\boldsymbol{\theta}$  has a probability density  $\pi_{\text{pr}}$ , which we also call the *prior*. Further, we consider a (possibly complicated) *parameter-to-event map*  $F : \Theta \rightarrow \mathbb{R}$ , which maps the random parameter vector  $\boldsymbol{\theta}$  to the quantity of interest or event outcome  $F(\boldsymbol{\theta})$ . We are interested in events  $\mathcal{F} := \{\boldsymbol{\theta} : F(\boldsymbol{\theta}) \geq z\}$ , where  $z \in \mathbb{R}$  is a given threshold that captures the extremeness or maximal allowance of the event. Our aim is to estimate the rare event

---

\*Revised March 2023.

**Funding:** Partially supported by the US National Science Foundation through grant DMS #1723211 and the Multidisciplinary University Research Initiatives (MURI) Program, Office of Naval Research (ONR) grant number N00014-19-1-2421.

<sup>†</sup>Department of Applied Physics and Applied Mathematics, Columbia University, NY ([st3503@columbia.edu](mailto:st3503@columbia.edu)).

<sup>‡</sup>Courant Institute of Mathematical Sciences, New York University, NY ([stadler@cims.nyu.edu](mailto:stadler@cims.nyu.edu)).

probability, also called probability of failure

$$(1.1) \quad p_{\mathcal{F}} := \mathbb{P}[\mathcal{F}] = \int_{\Theta} \mathbb{1}_{\mathcal{F}}(\boldsymbol{\theta}) \pi_{\text{pr}}(\boldsymbol{\theta}) d\boldsymbol{\theta} = \mathbb{E}_{\pi_{\text{pr}}}[\mathbb{1}_{\mathcal{F}}(\boldsymbol{\theta})],$$

where  $\mathbb{1}_{\mathcal{F}} : \Theta \rightarrow \{0, 1\}$  is the indicator function, i.e.,  $\mathbb{1}_{\mathcal{F}}(\boldsymbol{\theta}) = 1$  if  $\boldsymbol{\theta} \in \mathcal{F}$ , and  $\mathbb{1}_{\mathcal{F}}(\boldsymbol{\theta}) = 0$  else.

**1.1. Challenges and related literature.** Since the random parameter  $\boldsymbol{\theta}$  may be defined over a high-dimensional space and the map  $F$  may be complicated, e.g., involve the solution of a differential equation, analytic calculation of (1.1) is generally intractable. Monte Carlo methods are the standard approach to study complex systems that include uncertainty. The standard Monte Carlo estimator [27, 28] for  $p_{\mathcal{F}}$  is  $\hat{p}_{\mathcal{F}}^{\text{MC}} := \frac{1}{N} \sum_{i=1}^N \mathbb{1}_{\mathcal{F}}(\boldsymbol{\theta}_i)$ , where  $\{\boldsymbol{\theta}_i\}_{i=1}^N$  are random draws from  $\pi_{\text{pr}}$ . This estimator is unbiased since  $\mathbb{E}_{\pi_{\text{pr}}}[\hat{p}_{\mathcal{F}}^{\text{MC}}] = p_{\mathcal{F}}$ , and its variance is

$$(1.2) \quad \mathbb{V}_{\pi_{\text{pr}}}[\hat{p}_{\mathcal{F}}^{\text{MC}}] = \frac{1}{N} \mathbb{V}_{\pi_{\text{pr}}}[\mathbb{1}_{\mathcal{F}}(\boldsymbol{\theta})] = \frac{1}{N} (p_{\mathcal{F}} - p_{\mathcal{F}}^2).$$

The coefficient of variation, a measure for the accuracy of the estimator, is defined as the ratio between the standard deviation and the expectation, i.e.,

$$(1.3) \quad \widehat{\text{CV}}^{\text{MC}} = \frac{\sqrt{\mathbb{V}_{\pi_{\text{pr}}}[\hat{p}_{\mathcal{F}}^{\text{MC}}]}}{\mathbb{E}_{\pi_{\text{pr}}}[\hat{p}_{\mathcal{F}}^{\text{MC}}]} = \frac{1}{\sqrt{N}} \frac{\sqrt{p_{\mathcal{F}} - p_{\mathcal{F}}^2}}{p_{\mathcal{F}}} \approx \frac{1}{\sqrt{N}} \frac{1}{\sqrt{p_{\mathcal{F}}}}.$$

For linear or moderately nonlinear maps  $F$ , the target probability  $p_{\mathcal{F}}$  decays exponentially as  $z$  is increased [40]. Thus, to maintain the same error level, the sample size  $N$  would have to increase exponentially, making the Monte Carlo estimation (1.3) very costly. Thus, these methods are insufficient to explore probabilities of rare events, which are typically in the range of  $10^{-3}$ – $10^{-10}$ .

Various approaches to overcome the challenges arising in rare event probability estimation have been proposed, including parameter space decomposition, sequential sampling and multilevel splitting [1, 6, 14, 36, 41, 45]. In this work, we focus on importance sampling and thus restrict our discussion to the relevant literature. Importance sampling (IS) [3, 22, 27] decreases the required number of samples by choosing a biasing proposal distributions that reduces the variance of the estimator. The key to applying IS for rare event sampling is to find a good biasing density. While the form of the optimal biasing density is known, it cannot be used directly because of the unknown normalizing constant. One approach to find a good biasing density are cross-entropy (CE) methods, which find proposals by minimizing the Kullback-Leibler (KL) divergence between a parametrized density (usually from an exponential family) and the optimal biasing density [10, 18]. However, CE methods are typically limited to low-dimensional problems. This is because finding an optimal density is itself based on sample evaluations, and the number of required samples increases with the dimension. Recent work combines dimension reduction ideas from Bayesian inverse problems [47] with CE to overcome this challenge [42]. A related approach is followed in [46], where the authors also borrow ideas from Bayesian inference to define a maximum a posteriori (MAP) point in parameter space and to construct Gaussian distributions to be used as proposal densities for IS sampling.

The samples used to find parameterized CE proposals should be drawn from the parameter region around the rare event set. Finding these regions is difficult since typically one does

not have much prior knowledge about which parameters lead to rare events. Thus, adaptive procedures are used, in which one starts from an initial proposal, and iteratively updates the parametric proposal using samples and evaluations from the previous step. These procedures are called adaptive importance sampling (AIS) methods [4, 31], and CE is one method used in AIS for updating biasing densities.

Taking the perspective of large deviation theory (LDT) has also proven useful to estimate rare event probabilities in system with random components [11, 40] and to sample rare and large fluctuations in non-equilibrium stochastic PDE systems [16]. In this approach, one solves an optimization problem to find the most important point (also called instanton) in the rare event set. Knowledge of this point provides asymptotic information about small probabilities and may help to guide IS [16, 40]. Probability estimation of rare events is also related to reliability analysis in engineering [13, 25]. Methods used in this context are based on the point with largest probability density (typically of a Gaussian distribution), combined with set approximations based on Taylor expansions called first and second order reliability methods (FORM and SORM) [15, 34, 38]. IS methods based on the most probable point have also been proposed [22, 38].

**1.2. Approach.** The approach we propose in this paper combines several of the ideas reviewed above. It uses large deviation theory and a cross-entropy method to identify an optimal parametric biasing density for importance sampling. Since we target problems with high-dimensional parameter space, cross-entropy approaches can become inefficient. Thus, we use cross-entropy only in the subspace that is most important for estimating the rare event probability. To identify this subspace, we use derivative information of the parameter-to-event map at the large deviation optimizer. This step borrows geometric approximation ideas for rare event set from reliability analysis.

Overall, this results in an adaptive importance sampling scheme for rare event probability estimation in high dimensions. The method first solves a constrained optimization problem to find the LDT optimizer in random space. Using first- and second-order derivative information of the parameter-to-event map at the LDT optimizer, we identify a low-dimensional subspace in which we perform a cross-entropy method to identify an optimal Gaussian biasing density for importance sampling. Repeating this procedure, we obtain an adaptive multiple importance sampling method that reuses all samples taken in the process.

**1.3. Contributions and limitations.** The main contributions made in this paper are as follows: (1) We propose a method for rare event probability estimation that does not require smoothing of the indicator function in (1.1), and has no critical numerical parameters that must be tuned. (2) Our method requires derivatives of the parameter-to-event map only in the initial phase consisting of LDT optimization and identification of the low-dimensional subspace informing the failure probability. The cross-entropy adaptive sampling procedure is derivative-free. (3) After the initial LDT optimization, all evaluations of the parameter-to-event map in the adaptive importance sampling are used in the final probability estimation.

Our approach also has some limitations. (1) We assume that the prior is a multivariate Gaussian or the push-forward of a multivariate Gaussian. Large deviation theory allows for more general priors, but for non-Gaussian priors it may not be straightforward to identify a low-dimensional failure-informing subspace. (2) The proposed method requires solution of an

optimization problem which is assumed to have a unique minimizer. (3) The LDT-informed subspace we use does not have guaranteed certification properties. However, the choice of subspace does not affect the correctness of the solution as it is only used in the construction of the biasing density for importance sampling. (4) For one variant of the proposed adaptive importance sampler, one cannot prove that it has zero bias. However, in our experiments (and in related experiments in the literature), one does not observe significant bias.

**2. Preliminaries.** In this section, we summarize basic properties of importance sampling (IS) and cross-entropy (CE) methods, which provide a parametric approximation of the optimal biasing density for IS. We also highlight the limitations these methods have for rare events and high-dimensional parameter spaces, which will then be addressed by the methods presented in [subsection 3.1](#).

In this work, we assume that the random vectors  $\boldsymbol{\theta}$  are distributed according to a multivariate Gaussian distribution, i.e.,  $\pi_{\text{pr}}$  is a Gaussian density. This is a reasonable assumption in many applications. The methods we propose can easily be generalized to distributions that are push-forwards of multivariate Gaussians under a nonlinear map such as a Rosenblatt or Nataf transformation [25], or to Gaussian mixtures [2]. Since any finite-dimensional multivariate Gaussian can be linearly mapped to a standard multivariate normal  $\mathcal{N}(\mathbf{0}, \mathbf{I}_n)$ , we assume, without loss of generality, that  $\pi_{\text{pr}} \sim \mathcal{N}(\mathbf{0}, \mathbf{I}_n)$  for the remainder of this paper. We remark that in the context of failure probability estimation in engineering, it is common to define the *limit-state function (LSF)* as  $g(\boldsymbol{\theta}) := z - F(\boldsymbol{\theta})$ . Then, the failure set can be equivalently be written as  $\mathcal{F} = \{\boldsymbol{\theta} : g(\boldsymbol{\theta}) \leq 0\}$ .

**2.1. Importance sampling.** The ineffectiveness of standard MC for rare event probability estimation is due to the large number of samples  $\boldsymbol{\theta}_i$  that fall outside of  $\mathcal{F}$ , which implies that  $\mathbb{1}_{\mathcal{F}}(\boldsymbol{\theta}_i) = 0$ . The idea of importance sampling (IS) is to sample from a *proposal/biasing density*  $\pi_{\text{bias}}$  that has high density in the failure set  $\mathcal{F}$  rather than from the prior distribution. This can substantially increase the information provided by each sample evaluation [3, 22, 27]. The IS estimator is defined as

$$\hat{p}_{\mathcal{F}}^{\text{IS}} := \frac{1}{N} \sum_{i=1}^N \mathbb{1}_{\mathcal{F}}(\boldsymbol{\theta}_i) w(\boldsymbol{\theta}_i), \text{ with } w(\boldsymbol{\theta}_i) = \frac{\pi_{\text{pr}}(\boldsymbol{\theta}_i)}{\pi_{\text{bias}}(\boldsymbol{\theta}_i)},$$

where the samples  $\{\boldsymbol{\theta}_i\}_{i=1}^N \stackrel{\text{i.i.d.}}{\sim} \pi_{\text{bias}}$  are independent and identically distributed samples from a distribution with density  $\pi_{\text{bias}}$ . Specially, when the bias density is a Gaussian with mean  $\boldsymbol{\mu}$  and covariance  $\boldsymbol{\Sigma}$ , the IS weight has the explicit formula

$$(2.1) \quad w_{\text{GIS}}(\boldsymbol{\theta}; \boldsymbol{\mu}, \boldsymbol{\Sigma}) := (\det \boldsymbol{\Sigma})^{\frac{1}{2}} \exp \left( -\frac{1}{2} \|\boldsymbol{\theta}\|^2 + \frac{1}{2} \|\boldsymbol{\theta} - \boldsymbol{\mu}\|_{\boldsymbol{\Sigma}^{-1}}^2 \right).$$

The IS estimator  $\hat{p}_{\mathcal{F}}^{\text{IS}}$  is unbiased, i.e.,  $\mathbb{E}_{\pi_{\text{bias}}}[\hat{p}_{\mathcal{F}}^{\text{IS}}] = p_{\mathcal{F}}$ , provided that the support of the biasing density  $\pi_{\text{bias}}$  contains  $\mathcal{F}$ , which is true for Gaussian proposals. Its variance is

$$(2.2) \quad \mathbb{V}_{\pi_{\text{bias}}}[\hat{p}_{\mathcal{F}}^{\text{IS}}] = \frac{1}{N} \mathbb{V}_{\pi_{\text{bias}}}[\mathbb{1}_{\mathcal{F}}(\boldsymbol{\theta}) w(\boldsymbol{\theta})] = \frac{1}{N} (\mathbb{E}_{\pi_{\text{bias}}}[\mathbb{1}_{\mathcal{F}}(\boldsymbol{\theta}) w^2(\boldsymbol{\theta})] - p_{\mathcal{F}}^2).$$

The minimizer of  $\mathbb{V}_{\pi_{\text{bias}}}[\hat{p}_{\mathcal{F}}^{\text{IS}}]$  over all possible biasing densities  $\pi_{\text{bias}}$  is the optimal biasing density

$$(2.3) \quad \pi_{\mathcal{F}}(\boldsymbol{\theta}) := \frac{\mathbb{1}_{\mathcal{F}}(\boldsymbol{\theta})\pi_{\text{pr}}(\boldsymbol{\theta})}{\int \mathbb{1}_{\mathcal{F}}(\boldsymbol{\theta})\pi_{\text{pr}}(\boldsymbol{\theta})d\boldsymbol{\theta}} = \frac{1}{p_{\mathcal{F}}}\mathbb{1}_{\mathcal{F}}(\boldsymbol{\theta})\pi_{\text{pr}}(\boldsymbol{\theta}),$$

which provides a zero-variance IS estimator, i.e.,  $\mathbb{V}_{\pi_{\text{bias}}}[\hat{p}_{\mathcal{F}}^{\text{IS}}] = 0$  when  $\pi_{\text{bias}} = \pi_{\mathcal{F}}$ . However, it is impractical to use (2.3) for IS, because the normalizing constant  $p_{\mathcal{F}}$  is unknown; indeed, it is the target of the estimation problem. Although it is impossible to evaluate and sample directly from  $\pi_{\mathcal{F}}$ , this still provides a guide on how to choose an IS biasing distribution. Next, we summarize cross-entropy (CE) methods for obtaining approximations of  $\pi_{\mathcal{F}}$ , from which we can draw samples more easily.

**2.2. Cross-entropy method (CE).** As discussed above, the optimal biasing density  $\pi_{\mathcal{F}}$  in (2.3) is not available. The goal of cross-entropy methods [10, 35] is to find approximations for optimal biasing densities. CE methods approximate a target distribution  $\pi_{\text{bias}}^*$  (such as  $\pi_{\mathcal{F}}$  in our case) with a parametric biasing density  $\pi_{\text{bias}}(\boldsymbol{\theta}; \mathbf{v})$  with reference parameter  $\mathbf{v}$  by choosing from a family of densities  $\{\pi_{\text{bias}}(\cdot; \mathbf{v})\}$  the one that minimizes the Kullback-Leibler (KL) divergence  $D_{\text{KL}}(\pi_{\text{bias}}^* || \pi_{\text{bias}}(\boldsymbol{\theta}; \mathbf{v}))$ . This approximated distribution is then used to sample and evaluate the IS estimator. For Gaussian parametric biasing densities, the parameters  $\mathbf{v}$  are the mean  $\boldsymbol{\mu}$  and covariance matrix  $\boldsymbol{\Sigma}$ . From the definition of the KL divergence,

$$(2.4) \quad D_{\text{KL}}(\pi_{\text{bias}}^* || \pi_{\text{bias}}(\boldsymbol{\theta}; \mathbf{v})) = \mathbb{E}_{\pi_{\text{bias}}^*} \ln \left( \frac{\pi_{\text{bias}}^*(\boldsymbol{\theta})}{\pi_{\text{bias}}(\boldsymbol{\theta}; \mathbf{v})} \right) = \mathbb{E}_{\pi_{\text{bias}}^*} \ln \pi_{\text{bias}}^*(\boldsymbol{\theta}) - \mathbb{E}_{\pi_{\text{bias}}^*} \ln \pi_{\text{bias}}(\boldsymbol{\theta}; \mathbf{v}).$$

Since the first term on the right hand side above does not depend on  $\mathbf{v}$ , minimizing the KL divergence is equivalent to the following problem:

$$(2.5) \quad \mathbf{v}^* = \underset{\mathbf{v}}{\operatorname{argmax}} \mathbb{E}_{\pi_{\text{bias}}^*} [\ln \pi_{\text{bias}}(\boldsymbol{\theta}; \mathbf{v})] = \underset{\mathbf{v}}{\operatorname{argmax}} \mathbb{E}_{\pi_{\text{pr}}} [\ln \pi_{\text{bias}}(\boldsymbol{\theta}; \mathbf{v}) \mathbb{1}_{\mathcal{F}}(\boldsymbol{\theta})].$$

The expectation can be rewritten under the measure of another biasing density  $\pi'_{\text{bias}}(\cdot)$  and the corresponding IS weight  $w'(\cdot)$ , thus the maximization problem is equivalent to

$$(2.6) \quad \mathbf{v}^* = \underset{\mathbf{v}}{\operatorname{argmax}} \mathbb{E}_{\pi'_{\text{bias}}} [\ln \pi_{\text{bias}}(\boldsymbol{\theta}; \mathbf{v}) \mathbb{1}_{\mathcal{F}}(\boldsymbol{\theta}) w'(\boldsymbol{\theta})], \text{ with } w'(\boldsymbol{\theta}) = \frac{\pi_{\text{pr}}(\boldsymbol{\theta})}{\pi'_{\text{bias}}(\boldsymbol{\theta})}.$$

CE methods choose  $\pi'_{\text{bias}}(\cdot) = \pi_{\text{bias}}(\cdot; \mathbf{v}')$  from the same density family, start with an initial choice of  $\mathbf{v}'$  and iteratively update the reference parameter  $\mathbf{v}^*$  using (2.6).

For a Gaussian density  $\pi_{\text{bias}}(\boldsymbol{\theta}; [\boldsymbol{\mu}, \boldsymbol{\Sigma}]) = (2\pi)^{-\frac{n}{2}} (\det \boldsymbol{\Sigma})^{-\frac{1}{2}} \exp(-\frac{1}{2} \|\boldsymbol{\theta} - \boldsymbol{\mu}\|_{\boldsymbol{\Sigma}^{-1}}^2)$ , the optimal mean and covariance can be computed analytically from (2.6):

$$(2.7) \quad \boldsymbol{\mu}^* = \frac{\mathbb{E}_{\pi'_{\text{bias}}} [\mathbb{1}_{\mathcal{F}}(\boldsymbol{\theta}) w'(\boldsymbol{\theta}) \boldsymbol{\theta}]}{\mathbb{E}_{\pi'_{\text{bias}}} [\mathbb{1}_{\mathcal{F}}(\boldsymbol{\theta}) w'(\boldsymbol{\theta})]}, \quad \boldsymbol{\Sigma}^* = \frac{\mathbb{E}_{\pi'_{\text{bias}}} [\mathbb{1}_{\mathcal{F}}(\boldsymbol{\theta}) w'(\boldsymbol{\theta}) (\boldsymbol{\theta} - \boldsymbol{\mu}^*)(\boldsymbol{\theta} - \boldsymbol{\mu}^*)^{\top}]}{\mathbb{E}_{\pi'_{\text{bias}}} [\mathbb{1}_{\mathcal{F}}(\boldsymbol{\theta}) w'(\boldsymbol{\theta})]}.$$

Using samples  $\{\boldsymbol{\theta}_i\}_{i=1}^N \stackrel{\text{i.i.d.}}{\sim} \pi'_{\text{bias}}$ , the optimal mean and covariance  $\mathbf{v}^*$  can be calculated as [18]:

$$(2.8) \quad \boldsymbol{\mu}^* = \frac{\sum_{i=1}^N \mathbb{1}_{\mathcal{F}}(\boldsymbol{\theta}_i) w'(\boldsymbol{\theta}_i) \boldsymbol{\theta}_i}{\sum_{i=1}^N \mathbb{1}_{\mathcal{F}}(\boldsymbol{\theta}_i) w'(\boldsymbol{\theta}_i)}, \quad \boldsymbol{\Sigma}^* = \frac{\sum_{i=1}^N \mathbb{1}_{\mathcal{F}}(\boldsymbol{\theta}_i) w'(\boldsymbol{\theta}_i) (\boldsymbol{\theta}_i - \boldsymbol{\mu}^*)(\boldsymbol{\theta}_i - \boldsymbol{\mu}^*)^{\top}}{\sum_{i=1}^N \mathbb{1}_{\mathcal{F}}(\boldsymbol{\theta}_i) w'(\boldsymbol{\theta}_i)}.$$

From the above derivation, we identify three main challenges for the CE method when applied to high-dimensional problems with expensive-to-evaluate parameter-to-event maps:

- (1) To obtain useful estimates (2.8) of  $\boldsymbol{\mu}^*$  and  $\boldsymbol{\Sigma}^*$  with a moderate number of samples  $N$ , a good biasing density  $\pi'_{\text{bias}}$  is needed, for which a large fraction of evaluations  $\mathbb{1}_{\mathcal{F}}(\boldsymbol{\theta}_i)$  are nonzero and the weights  $w'(\boldsymbol{\theta}_i)$  are large.
- (2) When  $\boldsymbol{\theta}$  is high-dimensional, a large number of samples are required to estimate  $\boldsymbol{\mu}^*$  and  $\boldsymbol{\Sigma}^*$  in (2.8), even if a good biasing density  $\pi'_{\text{bias}}$  is available.
- (3) Samples  $\{\boldsymbol{\theta}_i\}_{i=1}^N \stackrel{\text{i.i.d.}}{\sim} \pi'_{\text{bias}}$  used to (iteratively) find optimal parameters  $\boldsymbol{v}^*$  are typically not used in the final estimator, which wastes expensive evaluations of  $\mathcal{F}$ . This also separates the method into a step to find the biasing density, and into the IS step to estimate the rare event probability. Thus, it requires to choose when to switch from one step to the other.

In [42], the authors tackle some of the above challenges. They address (1) using a sequence of smoothed approximations of  $\mathbb{1}_{\mathcal{F}}$  with a smoothing parameter  $s$  to increase the ratio of nonzero evaluations, and construct a failure-informed subspace to reduce the dimension of the problem, addressing (2). In particular, they start with the prior distribution as  $\pi'_{\text{bias}}$  and large  $s$  (i.e., a rather smooth approximation), obtain the low-dimensional subspace using gradient information of a smoothed version of  $\mathbb{1}_{\mathcal{F}}$  (details in subsection 3.2.1) and apply the CE method in this subspace. Then, they reduce  $s$  and use this newly-obtained proposal as  $\pi'_{\text{bias}}$  to update the subspace and the CE mean and covariance. This step is repeated until a good IS biasing density is found. This requires a substantial number of evaluations of  $F$  and  $\nabla F$  which are not used for the final probability computation. Additionally, the cost of this procedure increases with the rareness of the event. In the next section, we use ideas from large deviation theory to find an initial biasing density using optimization, addressing (1). We then use local derivative information at the optimizing point to identify a low-dimensional subspace, addressing (2). Since we do not require smoothing, our method involves few parameters and uses all evaluations of  $F$  in the sampling step for the probability estimation by employing a multiple IS method, addressing (3).

**3. LDT-based adaptive importance sampling.** In this section, we show how large deviation theory can provide an initial biasing density for adaptive importance sampling (subsection 3.1). Moreover, LDT also provides dimension reduction information required to apply CE methods in a subspace only (subsection 3.2). Combining these ideas, we propose a multiple IS algorithm for the target probability that reuses all evaluations of  $F$  in the sampling step and thus seamlessly merges the parametric biasing density optimization and the probability estimation phases.

**3.1. Large deviation theory (LDT).** Large deviation theory is a classical theory on the asymptotic behavior of sequences of probability distributions [12, 43]. Recent studies adapt LDT to systems with random parameters and build connections between extreme event probability estimation and constrained optimization [11, 39, 40]. LDT states that the least-unlikely point  $\boldsymbol{\theta}^*$  in the event set  $\mathcal{F}$  carries important information about  $p_{\mathcal{F}}$ . We refer to  $\boldsymbol{\theta}^*$  as the LDT optimizer, and it is the solution of the constrained optimization problem

$$(3.1) \quad \boldsymbol{\theta}^* := \underset{\boldsymbol{\theta} \in \mathcal{F}}{\operatorname{argmin}} I(\boldsymbol{\theta}),$$

where the rate function  $I$  depends only on  $\pi_{\text{pr}}$ . For the standard normal case  $\mathcal{N}(\mathbf{0}, \mathbf{I}_n)$ , the rate function is simply  $I(\boldsymbol{\theta}) = \frac{1}{2}\|\boldsymbol{\theta}\|^2$ . Then, LDT shows that under reasonable regularity conditions on  $F$ , the probability  $p_{\mathcal{F}}$  is log-asymptotic to  $\exp(-I(\boldsymbol{\theta}^*))$ , i.e.,  $\ln p_{\mathcal{F}} \rightarrow -I(\boldsymbol{\theta}^*)$  as  $z \rightarrow \infty$ . Using this directly is limited due to the occurrence of the logarithm and due to its asymptotic nature, i.e., it only holds in the limit as the probability tends to zero. Significant research has been performed to improve this log-asymptotic estimate through estimation of prefactors either in the context of stochastic differential equations [16, 19, 37] or systems with uncertain parameters [11, 40].

The LDT optimizer  $\boldsymbol{\theta}^*$  induces a proposal for an IS method that is centered at  $\boldsymbol{\theta}^*$ . That proposal is  $\mathcal{N}(\boldsymbol{\theta}^*, \mathbf{I}_n)$ , and the corresponding LDT-based shifted importance sampling (LSIS) estimator is

$$(3.2) \quad \hat{p}_{\mathcal{F}}^{\text{LSIS}} := \frac{1}{N} \sum_{i=1}^N \mathbb{1}_{\mathcal{F}}(\boldsymbol{\theta}_i) w_{\text{LSIS}}(\boldsymbol{\theta}_i), \text{ with } w_{\text{LSIS}}(\boldsymbol{\theta}_i) := w_{\text{GIS}}(\boldsymbol{\theta}_i; \boldsymbol{\theta}^*, \mathbf{I}_n),$$

where  $\{\boldsymbol{\theta}_i\}_{i=1}^N \stackrel{\text{i.i.d.}}{\sim} \mathcal{N}(\boldsymbol{\theta}^*, \mathbf{I}_n)$  are samples from the shifted prior, and  $w_{\text{GIS}}$  is defined in (2.1). For linear or moderately nonlinear  $F$  and for extreme events (large  $z$  and small  $p_{\mathcal{F}}$ ), the error of the LSIS estimator is reduced by an exponential term compared with standard Monte Carlo methods [40]. For severely nonlinear problems in high dimensions, this method might underestimate the probability due to a large number of zero evaluations of the indicator function at the generated samples [23]. In the context of SDEs, the optimizer (3.1) is also called *instanton*, and can be used to form an alternative SDE which allows to sample, e.g., large fluctuations in non-equilibrium systems [16]. The resulting instanton-based importance sampling method is analogous to LSIS. LSIS serves as a good initial choice of the biasing density  $\pi'_{\text{bias}} = \pi_{\text{LSIS}}$ , acting as alternative to using smooth approximations of the indicator function as in [42] to avoid a large number of zero evaluations of  $\mathbb{1}_{\mathcal{F}}$ .

**3.2. Dimension reduction.** As discussed in subsection 2.2, the effectiveness of cross-entropy methods depends crucially on the choice of the biasing distribution used to compute the reference parameters. As can be seen in (2.8), each sample updates the covariance matrix approximation by at most a rank-1 matrix. Since the covariance must be positive and the approximations of the mean and covariance sufficiently accurate, one typically needs  $N_{\text{CE}} \gg n$  samples, where  $n$  is the dimension of the parameter space and  $N_{\text{CE}}$  is the sample size used in the CE method for finding optimal reference parameters. When  $n$  is large and evaluation of  $F$  is costly, using CE might thus not be practical. However, rare event probability estimation problems often have intrinsic low-dimensional structure, resulting from properties of the parameter-to-event map and correlation of the random parameters. We exploit such structure by tailoring the biasing distribution  $\pi_{\text{bias}}$  in the low-dimensional subspace using the CE method, thus drastically reducing the number of required samples. In the next section, we use the relationship between rare event probability estimation and Bayesian inference, allowing the transfer of dimension reduction ideas from the latter to the former. In subsection 3.2.2, we use ideas from LDT to identify an appropriate low-dimensional space that is informative for rare events, and in subsection 3.2.3 we show how to use CE in that subspace.

**3.2.1. Low-dimensional subspace informing rare event probability.** Assume there is a low-dimensional subspace of the random parameter space that is important for the rare event probability estimation. Before discussing how to find such a space, we show how, once available, it can be used. We assume an orthonormal basis of  $\mathbb{R}^n$  such that this subspace is spanned by the columns of  $\mathbf{\Phi}_r \in \mathbb{R}^{n \times r}$ , and the columns of  $\mathbf{\Phi}_\perp \in \mathbb{R}^{n \times (n-r)}$  are the remaining orthonormal basis vectors. This induces the orthogonal decomposition  $\boldsymbol{\theta} = \mathbf{\Phi}_r \mathbf{\Phi}_r^\top \boldsymbol{\theta} + \mathbf{\Phi}_\perp \mathbf{\Phi}_\perp^\top \boldsymbol{\theta} = \mathbf{\Phi}_r \tilde{\boldsymbol{\theta}}_r + \mathbf{\Phi}_\perp \tilde{\boldsymbol{\theta}}_\perp$ , where  $\tilde{\boldsymbol{\theta}} = [\tilde{\boldsymbol{\theta}}_r, \tilde{\boldsymbol{\theta}}_\perp] \in \mathbb{R}^n$  has the components  $\tilde{\boldsymbol{\theta}}_r := \mathbf{\Phi}_r^\top \boldsymbol{\theta} \in \mathbb{R}^r$  and  $\tilde{\boldsymbol{\theta}}_\perp := \mathbf{\Phi}_\perp^\top \boldsymbol{\theta} \in \mathbb{R}^{n-r}$  are the coordinates of  $\boldsymbol{\theta}$  for the basis  $\mathbf{\Phi} := [\mathbf{\Phi}_r, \mathbf{\Phi}_\perp]$ .

Partially motivated by dimension reduction ideas from Bayesian inverse problem, i.e., considering  $\pi_{\mathcal{F}}$  as a posterior density and  $\mathbb{1}_{\mathcal{F}}(\boldsymbol{\theta})$  as the likelihood, the optimal low-dimensional density  $\pi_{\mathcal{F}}^r$  for a subspace with basis  $\mathbf{\Phi}_r$  can be obtained by minimizing the KL divergence  $D_{\text{KL}}(\pi_{\mathcal{F}} || \pi_{\mathcal{F}}^r)$ , resulting in, [42, 47]

$$(3.3) \quad \pi_{\mathcal{F}}^r(\boldsymbol{\theta}) \propto \mathbb{E}_{\pi_{\text{pr}}}[\mathbb{1}_{\mathcal{F}}(\boldsymbol{\theta}) | \mathbf{\Phi}_r \mathbf{\Phi}_r^\top \boldsymbol{\theta}] \pi_{\text{pr}}(\boldsymbol{\theta}),$$

where the conditional expectation is defined as

$$\mathbb{E}_{\pi_{\text{pr}}}[\mathbb{1}_{\mathcal{F}}(\boldsymbol{\theta}) | \mathbf{\Phi}_r \mathbf{\Phi}_r^\top \boldsymbol{\theta}] := \int_{\mathbb{R}^{n-r}} \mathbb{1}_{\mathcal{F}}(\mathbf{\Phi}_r \mathbf{\Phi}_r^\top \boldsymbol{\theta} + \mathbf{\Phi}_\perp \tilde{\boldsymbol{\theta}}_\perp) \frac{\pi_{\text{pr}}(\mathbf{\Phi}_r \mathbf{\Phi}_r^\top \boldsymbol{\theta} + \mathbf{\Phi}_\perp \tilde{\boldsymbol{\theta}}_\perp)}{\int_{\mathbb{R}^{n-r}} \pi_{\text{pr}}(\mathbf{\Phi}_r \mathbf{\Phi}_r^\top \boldsymbol{\theta} + \mathbf{\Phi}_\perp \tilde{\boldsymbol{\theta}}'_\perp) d\tilde{\boldsymbol{\theta}}'_\perp} d\tilde{\boldsymbol{\theta}}_\perp.$$

The remaining question is how to choose the subspace and its basis  $\mathbf{\Phi}_r$ . In [42], the authors use the failure-informed subspace (FIS), which is computed from the generalized eigenvalues of the matrix

$$(3.4) \quad \mathbf{H}_{\text{FIS}} := \mathbb{E}_{\pi_{\mathcal{F}}} \nabla \ln f(\boldsymbol{\theta}; s) \nabla \ln f(\boldsymbol{\theta}; s)^\top,$$

where  $f(\boldsymbol{\theta}; s)$  is a smooth approximation of  $\mathbb{1}_{\mathcal{F}}(\boldsymbol{\theta})$ , e.g.,  $f(\boldsymbol{\theta}; s) := \frac{1}{2} [1 + \tanh((F(\boldsymbol{\theta}) - z)/s)]$ . The dominant generalized eigenvectors of  $\mathbf{H}_{\text{FIS}}$  form the columns of  $\mathbf{\Phi}_r$ . This approach adopts dimension reduction methods originally developed for Bayesian inverse problems in [47], for which certified error bound for  $D_{\text{KL}}(\pi_{\mathcal{F}} || \pi_{\mathcal{F}}^r)$  are available. The corresponding cross-entropy-based IS with failure-informed dimension reduction is termed iCEred in [42]. We will compare the performance of this method to the approach we propose in this paper.

Alternative dimension reduction methods, namely local and global likelihood-informed subspaces (LIS) are proposed in the context of Bayesian inverse problems in [8]. Motivated by the Bayesian linear-Gaussian model, these approaches use the subspace spanned by the dominant eigenvectors of the Gauss-Newton Hessian of the negative log-likelihood (either at a point or integrated over the posterior  $\pi_{\mathcal{F}}$ ). These LIS projectors do not come with certified error bounds for the resulting posterior approximation. Both the certified dimension reduction using the dominant eigenspace of the matrix (3.4) and the global LIS methodologies perform comparably well in applications for nonlinear Bayesian inverse problems [47].

**3.2.2. LDT-informed subspace.** Dimension reduction based on (3.4) and the global LIS method both require sampling over the posterior  $\pi_{\mathcal{F}}$  and evaluation of derivatives to build the low-rank projector. We would like to limit the number of evaluations of  $F$  and its derivatives as these typically dominate the computational cost. For that purpose, we use geometric information at the LDT optimizer (see subsection 3.1) and a local LIS approach to identify

a low-dimensional subspace, building on the result that one can asymptotically approximate the rare event probability by using local derivative information at the LDT optimizer. In the engineering literature, a similar perspective is referred to as the second-order reliability method (SORM) [15]. For reference, we summarize a result from [40] here.

**Theorem 3.1 (Second-order approximation).** *Let  $\boldsymbol{\theta} \sim \mathcal{N}(\mathbf{0}, \mathbf{I}_n)$  and assume that  $F$  is twice continuously differentiable. Denote by  $\boldsymbol{\theta}^*$  the optimizer of (3.1), and assume that the minimizer  $\boldsymbol{\theta}^*$  satisfies a second-order sufficient optimality condition, i.e.,  $\mathbf{I}_n - \lambda \nabla^2 F(\boldsymbol{\theta}^*)$  is positive definite, where  $\lambda := \|\nabla I(\boldsymbol{\theta}^*)\|/\|\nabla F(\boldsymbol{\theta}^*)\|$ . Denote the normal direction at  $\boldsymbol{\theta}^*$  as  $\hat{\mathbf{n}} := \nabla F(\boldsymbol{\theta}^*)/\|\nabla F(\boldsymbol{\theta}^*)\|$ . Then, an approximation  $\hat{p}_{\mathcal{F}}^{\text{SO}}$  of  $p_{\mathcal{F}}$  using a second-order approximation of the rare event set can be computed as*

$$(3.5) \quad \hat{p}_{\mathcal{F}}^{\text{SO}} := \frac{(2\pi)^{-\frac{1}{2}}}{\sqrt{2I(\boldsymbol{\theta}^*)}} \prod_{i=1}^n [1 - \lambda \lambda_i(\mathbf{H}_{\text{LDT}})]^{-\frac{1}{2}} \exp(-I(\boldsymbol{\theta}^*)),$$

where

$$(3.6) \quad \mathbf{H}_{\text{LDT}} := (\mathbf{I}_n - \hat{\mathbf{n}}\hat{\mathbf{n}}^\top) \nabla^2 F(\boldsymbol{\theta}^*) (\mathbf{I}_n - \hat{\mathbf{n}}\hat{\mathbf{n}}^\top)$$

is the Hessian of  $F$  at  $\boldsymbol{\theta}^*$  projected onto the hyperplane orthogonal to  $\hat{\mathbf{n}}$ , and  $\lambda_i(\mathbf{H}_{\text{LDT}})$  is its  $i$ -th eigenvalue. Moreover, this approximation is asymptotic to  $p_{\mathcal{F}}$ , i.e.,  $\hat{p}_{\mathcal{F}}^{\text{SO}} \rightarrow p_{\mathcal{F}}$  as  $z \rightarrow \infty$ .

For fixed  $\boldsymbol{\theta}^*$ , we observe that the values contributing most to the product in (3.5) are  $\lambda$ , which is related to the gradient norm  $\|\nabla F(\boldsymbol{\theta}^*)\|$ , and the dominating eigenvalues of  $\mathbf{H}_{\text{LDT}}$ . This suggests that  $\hat{\mathbf{n}}$  and the corresponding eigenvectors of  $\mathbf{H}_{\text{LDT}}$  are important directions for the rare event probability.

As we will show next, this observation can be confirmed by using the relation between rare event probability estimation and Bayesian inverse problems and following similar steps as in [42]. In Bayesian inference, dimension reduction is based on the goal to identify the subspace that is most important for the update from the prior to the posterior. As in [42], to avoid the discontinuity of the indicator function  $\mathbb{1}_{\mathcal{F}}(\boldsymbol{\theta})$ , we introduce a smooth approximation with smoothing parameter  $s > 0$ ,

$$(3.7) \quad f(\boldsymbol{\theta}; s) := \frac{1}{2} \left[ 1 + \tanh \left( \frac{F(\boldsymbol{\theta}) - z}{s} \right) \right], \text{ where } \lim_{s \rightarrow 0} f(\boldsymbol{\theta}; s) = \mathbb{1}_{\mathcal{F}}(\boldsymbol{\theta}).$$

Thus, the negative log-likelihood is approximated as  $-\ln f(\boldsymbol{\theta}; s) = \ln 2 - \ln [1 + \tanh((F(\boldsymbol{\theta}) - z)/s)]$ . We now compute derivatives with respect to  $\boldsymbol{\theta}$ . Using the notation  $\alpha(\boldsymbol{\theta}; s) := 1 - \tanh((F(\boldsymbol{\theta}) - z)/s)$ , the gradient and Hessian are

$$(3.8) \quad \nabla(-\ln f(\boldsymbol{\theta}; s)) = -\frac{\alpha(\boldsymbol{\theta}; s)}{s} \nabla F(\boldsymbol{\theta})$$

$$(3.9) \quad \nabla^2(-\ln f(\boldsymbol{\theta}; s)) = -\frac{\alpha(\boldsymbol{\theta}; s)}{s} \nabla^2 F(\boldsymbol{\theta}) + \frac{2\alpha(\boldsymbol{\theta}; s) - \alpha^2(\boldsymbol{\theta}; s)}{s^2} \nabla F(\boldsymbol{\theta}) \nabla F(\boldsymbol{\theta})^\top.$$

In [42], the authors derive a low-dimensional failure-informed subspace by sampling the gradients (3.8) with fixed regularization parameter  $s$  to approximate (3.4). They use the dominating eigenvalue directions of the resulting second moment matrix to compute the low-dimensional, failure-informed subspace and repeat this procedure for decreasing  $s > 0$ . An

alternative approach to dimension reduction is using the likelihood-informed subspace (LIS), which is spanned by the dominant eigenvectors of the Gauss-Newton Hessian of the negative log-likelihood [8]. Averaging of Hessians over the posterior density leads to the global LIS method, while using the Hessian at a point amounts to the local LIS method. We use the latter here and evaluate the Hessian at the LDT optimizer  $\boldsymbol{\theta}^*$ . This is also motivated by large deviation theory, which shows that the probability measure concentrates around  $\boldsymbol{\theta}^*$  as  $z \rightarrow \infty$ .

To study the dominating eigenvalues of the Hessian (3.9) for  $\boldsymbol{\theta} = \boldsymbol{\theta}^*$  and as  $s \rightarrow 0$ , note that  $\alpha(\boldsymbol{\theta}^*, s) = 1$  independent of  $s$ . Thus, for sufficiently small  $s$ , the first term in (3.9) is dominated by the second. As a consequence,  $\nabla F(\boldsymbol{\theta}^*)$  is a dominating eigenvector direction of the Hessian (3.9) and should thus be in the local LIS. Let us now consider directions that are orthogonal to  $\nabla F(\boldsymbol{\theta}^*)$ . These directions are in the nullspace of the second term in (3.9), and thus the dominating directions are the dominating eigenvectors of  $\nabla^2 F(\boldsymbol{\theta}^*)$  in the hyperplane orthogonal to  $\hat{\boldsymbol{n}}$ . These can be computed as dominant eigenvectors of  $\mathbf{H}_{\text{LDT}}$  defined in (3.6), i.e., the same information as appears in Theorem 3.1.

To summarize, the local LIS is spanned by  $\nabla F(\boldsymbol{\theta}^*)$  (or equivalently, its normalized version  $\hat{\boldsymbol{n}}$ ) and the dominating eigenvectors of  $\mathbf{H}_{\text{LDT}}$ , which are both independent of  $s$ . Note that this definition only requires derivative information of  $F$  at the LDT optimizer  $\boldsymbol{\theta}^*$ . Using the notation from subsection 3.2.1, the subspace basis vectors form the columns of  $\boldsymbol{\Phi}_r$ . The first column is the normal direction  $\hat{\boldsymbol{n}}$ , and the other columns are the dominating eigenvectors of  $\mathbf{H}_{\text{LDT}}$ . The decay of the eigenvalues of  $\mathbf{H}_{\text{LDT}}$  can be used together with the value of  $\lambda$  to choose the rank  $r$  of the low-dimensional subspace. For example, we can choose  $r$  such that

$$(3.10) \quad \lambda \max_{i>r} |\lambda_i(\mathbf{H}_{\text{LDT}})| \leq \epsilon,$$

where  $\epsilon$  is a given threshold. In practice, we do not build the full matrix  $\mathbf{H}_{\text{LDT}}$ , but instead use its application to vectors and Lanczos or randomized SVD methods to find the dominating eigenvectors [9, 20]. The number of required matrix-vector applications for these methods is typically only moderately larger than the number of dominant eigenvalues.

**3.2.3. CE in low-dimensional subspace.** We now show how to use CE methods for approximating the optimal low-dimensional biasing density  $\pi_{\mathcal{F}}^*$ . This section largely follows [42] but we provide a summary for completeness. Using (3.3), we define the target density as

$$(3.11) \quad \pi_{\text{bias}}^*(\tilde{\boldsymbol{\theta}}) := \pi_{\mathcal{F}}^r(\boldsymbol{\theta}) \propto \mathbb{E}_{\pi_{\text{pr}}}[\mathbb{1}_{\mathcal{F}}(\boldsymbol{\theta}) | \boldsymbol{\Phi}_r \tilde{\boldsymbol{\theta}}_r] \pi_{\text{pr}}^r(\tilde{\boldsymbol{\theta}}_r) \pi_{\text{pr}}^\perp(\tilde{\boldsymbol{\theta}}_\perp),$$

where  $\boldsymbol{\theta} = \boldsymbol{\Phi} \tilde{\boldsymbol{\theta}}$  and we use that the prior distribution can be factorized as  $\pi_{\text{pr}}(\boldsymbol{\theta}) = \pi_{\text{pr}}^r(\tilde{\boldsymbol{\theta}}_r) \pi_{\text{pr}}^\perp(\tilde{\boldsymbol{\theta}}_\perp)$ . Similarly, the parametric biasing density is defined as

$$(3.12) \quad \pi_{\text{bias}}(\tilde{\boldsymbol{\theta}}; \mathbf{v}_r) := \pi_{\text{bias}}^r(\tilde{\boldsymbol{\theta}}_r; \mathbf{v}_r) \pi_{\text{pr}}^\perp(\tilde{\boldsymbol{\theta}}_\perp),$$

where  $\mathbf{v}_r$  represents the mean and covariance in the  $r$ -dimensional subspace.

To apply CE to minimize  $D_{\text{KL}}(\pi_{\text{bias}}^* || \pi_{\text{bias}})$  using (3.11) and (3.12), we solve the following

problem [42],

$$\begin{aligned}
\mathbf{v}_r^* &= \operatorname{argmax}_{\mathbf{v}_r} \mathbb{E}_{\pi_{\text{bias}}^*} [\ln \pi_{\text{bias}}(\tilde{\boldsymbol{\theta}}; \mathbf{v}_r)] = \operatorname{argmax}_{\mathbf{v}_r} \mathbb{E}_{\pi_{\text{bias}}^*} [\ln \pi_{\text{bias}}^r(\tilde{\boldsymbol{\theta}}; \mathbf{v}_r)] \\
&= \operatorname{argmax}_{\mathbf{v}_r} \int_{\mathbb{R}^r} [\ln \pi_{\text{bias}}^r(\tilde{\boldsymbol{\theta}}; \mathbf{v}_r)] \pi_{\text{pr}}^r(\tilde{\boldsymbol{\theta}}) \mathbb{E}_{\pi_{\text{pr}}} [\mathbb{1}_{\mathcal{F}}(\boldsymbol{\theta}) | \boldsymbol{\Phi}_r \tilde{\boldsymbol{\theta}}_r] \left( \int_{\mathbb{R}^{n-r}} \pi_{\text{pr}}^\perp(\tilde{\boldsymbol{\theta}}_\perp) d\tilde{\boldsymbol{\theta}}_\perp \right) d\tilde{\boldsymbol{\theta}}_r \\
&= \operatorname{argmax}_{\mathbf{v}_r} \int_{\mathbb{R}^r} [\ln \pi_{\text{bias}}^r(\tilde{\boldsymbol{\theta}}; \mathbf{v}_r)] \pi_{\text{pr}}^r(\tilde{\boldsymbol{\theta}}) \mathbb{E}_{\pi_{\text{pr}}} [\mathbb{1}_{\mathcal{F}}(\boldsymbol{\theta}) | \boldsymbol{\Phi}_r \tilde{\boldsymbol{\theta}}_r] d\tilde{\boldsymbol{\theta}}_r \\
(3.13) \quad &= \operatorname{argmax}_{\mathbf{v}_r} \int_{\mathbb{R}^r} [\ln \pi_{\text{bias}}^r(\tilde{\boldsymbol{\theta}}; \mathbf{v}_r)] \pi_{\text{pr}}^r(\tilde{\boldsymbol{\theta}}) \left( \int_{\mathbb{R}^{n-r}} \mathbb{1}_{\mathcal{F}}(\boldsymbol{\Phi}_r \tilde{\boldsymbol{\theta}}_r + \boldsymbol{\Phi}_\perp \tilde{\boldsymbol{\theta}}_\perp) \pi_{\text{pr}}^\perp(\tilde{\boldsymbol{\theta}}_\perp) d\tilde{\boldsymbol{\theta}}_\perp \right) d\tilde{\boldsymbol{\theta}}_r \\
&= \operatorname{argmax}_{\mathbf{v}_r} \int_{\mathbb{R}^n} \mathbb{1}_{\mathcal{F}}(\boldsymbol{\Phi}_r \tilde{\boldsymbol{\theta}}_r + \boldsymbol{\Phi}_\perp \tilde{\boldsymbol{\theta}}_\perp) [\ln \pi_{\text{bias}}^r(\tilde{\boldsymbol{\theta}}; \mathbf{v}_r)] \pi_{\text{pr}}(\tilde{\boldsymbol{\theta}}) d\tilde{\boldsymbol{\theta}} \\
&= \operatorname{argmax}_{\mathbf{v}_r} \mathbb{E}_{\pi_{\text{pr}}} [\mathbb{1}_{\mathcal{F}}(\boldsymbol{\theta}) \ln \pi_{\text{bias}}^r(\tilde{\boldsymbol{\theta}}; \mathbf{v}_r)].
\end{aligned}$$

Again, we can use another  $r$ -dimensional biasing density  $\pi'_{\text{bias}}$  with IS weights  $w'(\tilde{\boldsymbol{\theta}}_r) = \pi_{\text{pr}}^r(\tilde{\boldsymbol{\theta}}_r)/\pi'_{\text{bias}}(\tilde{\boldsymbol{\theta}}_r)$  to evaluate the expectation in the last term of (3.13). Thus, the optimal mean and covariance for the Gaussian proposal  $\pi_{\text{bias}}^r$  in the low-dimensional subspace are

$$(3.14) \quad \boldsymbol{\mu}_r^* = \frac{\sum_{i=1}^N \mathbb{1}_{\mathcal{F}}(\boldsymbol{\theta}_i) w'(\tilde{\boldsymbol{\theta}}_{r,i}) \tilde{\boldsymbol{\theta}}_{r,i}}{\sum_{i=1}^N \mathbb{1}_{\mathcal{F}}(\boldsymbol{\theta}_i) w'(\tilde{\boldsymbol{\theta}}_{r,i})}, \quad \boldsymbol{\Sigma}_r^* = \frac{\sum_{i=1}^N \mathbb{1}_{\mathcal{F}}(\boldsymbol{\theta}_i) w'(\tilde{\boldsymbol{\theta}}_{r,i}) (\tilde{\boldsymbol{\theta}}_{r,i} - \boldsymbol{\mu}_r) (\tilde{\boldsymbol{\theta}}_{r,i} - \boldsymbol{\mu}_r)^\top}{\sum_{i=1}^N \mathbb{1}_{\mathcal{F}}(\boldsymbol{\theta}_i) w'(\tilde{\boldsymbol{\theta}}_{r,i})},$$

where  $\tilde{\boldsymbol{\theta}}_{r,i} \stackrel{\text{i.i.d.}}{\sim} \pi'_{\text{bias}}$ ,  $\tilde{\boldsymbol{\theta}}_{\perp,i} \stackrel{\text{i.i.d.}}{\sim} \pi_{\text{pr}}^\perp$  and  $\boldsymbol{\theta}_i = \boldsymbol{\Phi}_r \tilde{\boldsymbol{\theta}}_{r,i} + \boldsymbol{\Phi}_\perp \tilde{\boldsymbol{\theta}}_{\perp,i}$ .

**3.3. Multiple and adaptive importance sampling.** In the previous sections, we discussed using LSIS as initial biasing proposal  $\pi'_{\text{bias}} = \pi_{\text{LSIS}}$  to estimate the mean and covariance of the optimal Gaussian proposal. In this step, we already evaluate the parameter-to-event map at several samples. Naturally, the question arises if we can reuse these samples in the IS, which leads to multiple importance sampling (MIS) methods. We can also apply MIS in the CE estimation step, i.e., we reuse all previous evaluations of  $F$  in sampling to iteratively update the CE mean and covariance. Repeated application of this procedure results in an adaptive importance sampling method [4, 31], whose adaptation to (1.1) is described next.

Multiple importance sampling (MIS) combines the independent samples from different proposal distributions and builds a new IS estimator as a weighted combination of different IS estimators [21, 30, 44]. For the problem we consider here, assume we have  $J$  proposals as  $\{\pi_j\}_{j=1}^J$  and  $N_j$  independent samples from each proposal  $\{\boldsymbol{\theta}_i^{(j)}\}_{i=1}^{N_j} \stackrel{\text{i.i.d.}}{\sim} \pi_j$ , and we denote the total number of samples as  $N = \sum_{j=1}^J N_j$  and assume that the IS weight formula for each proposal is  $w_j(\boldsymbol{\theta}) = \pi_{\text{pr}}(\boldsymbol{\theta})/\pi_j(\boldsymbol{\theta})$ . The MIS estimator is defined as

$$(3.15) \quad \hat{p}_{\mathcal{F}}^{\text{MIS}} = \frac{1}{N} \sum_{j=1}^J \sum_{i=1}^{N_j} \mathbb{1}_{\mathcal{F}}(\boldsymbol{\theta}_i^{(j)}) w_{\text{MIS}}(\boldsymbol{\theta}_i^{(j)}),$$

where weights  $w_{\text{MIS}}$  are computed using one of the following two strategies.

*Standard MIS (s-MIS)*. This approach uses the same weights as IS estimator for each individual proposal [5]. Thus, the MIS estimator  $\hat{p}_{\mathcal{F}}^{\text{MIS}}$  with standard proposal weights can be viewed as a weighted average of different IS estimators, with weights proportional to  $N_j$ :

$$(3.16) \quad w_{\text{s-MIS}}(\boldsymbol{\theta}_i^{(j)}) := \frac{\pi_{\text{pr}}(\boldsymbol{\theta}_i^{(j)})}{\pi_j(\boldsymbol{\theta}_i^{(j)})} = w_j(\boldsymbol{\theta}_i^{(j)}).$$

*Deterministic mixture MIS (dm-MIS)*. This approach uses weights defined as, [30],

$$(3.17) \quad w_{\text{DM-MIS}}(\boldsymbol{\theta}_i^{(j)}) := \pi_{\text{pr}}(\boldsymbol{\theta}_i^{(j)}) \Big/ \sum_{j'=1}^J \frac{N_{j'}}{N} \pi_{j'}(\boldsymbol{\theta}_i^{(j)}) = N \Big/ \sum_{j'=1}^J \frac{N_{j'}}{w_{j'}(\boldsymbol{\theta}_i^{(j)})}.$$

It can be shown that this dm-MIS estimator has a variance that is smaller than the variance of any weighting scheme, plus a term that goes to zero as  $\min\{N_j\} \rightarrow \infty$ , [44]. One can also view  $\hat{p}_{\mathcal{F}}^{\text{MIS}}$  with deterministic mixture weights as an IS estimator using the biasing density  $\pi_{\text{MIS}}$ , which is a weighted mixture distribution of  $\{\pi_j\}_{j=1}^J$ , i.e.,

$$(3.18) \quad \pi_{\text{MIS}}(\boldsymbol{\theta}) := \sum_{j'=1}^J \frac{N_{j'}}{N} \pi_{j'}(\boldsymbol{\theta}).$$

In our adaptive importance sampling method, we reuse all evaluations of the parameter-to-event map  $\{\mathbb{1}_{\mathcal{F}}(\boldsymbol{\theta}_i^{(j)})\}_{i,j}$  together with the weights  $\{w_j(\boldsymbol{\theta}_i^{(j)})\}_{i,j}$  to compute  $\hat{p}_{\mathcal{F}}^{\text{MIS}}$ . Moreover, we reuse all available sample evaluations and weights in each step of the CE method to update the Gaussian proposal. Thus, the updated proposal  $\pi_j$  depends on the previous samples. The s-MIS estimator stays unbiased [5], while the DM-MIS estimator might have a bias due to the loss of independency between samples from different proposals [7]. Although the dm-MIS estimator cannot be proven to be unbiased, it generally outperforms other AIS methods and has smaller errors in numerical experiments [7]. We also observe this in our numerical tests, in which we compare results obtained with s-MIS and dm-MIS weights.

The steps of the proposed LDT-based adaptive sampling method (LAIS) are visualized in two dimensions in [Figure 1](#). We start with a single proposal  $\pi_{\text{LSIS}}$ , and repeatedly use MIS to reuse the previous samples and corresponding evaluations to obtain an updated proposal using CE. Combined with the LDT-informed dimension reduction, the initialization ( $\pi_{\text{LSIS}}$  projected in the low-dimensional subspace), sampling and updates are conducted only in the low-dimensional subspace. This results in an adaptive multiple importance sampling scheme for rare event probability estimation, which is summarized in [Algorithm 3.1](#). The first steps ([Lines 2 and 3](#)) in this algorithm correspond to solving the LDT optimization problem [\(3.1\)](#) and finding a low-dimensional subspace as discussed in [subsection 3.2.2](#). Adaptive importance sampling in this low-dimensional space is based on the CE method and multiple importance sampling. The difference between LAIS-s and LAIS-dm lies in the computation of the MIS weights. For LAIS-s, the weights are computed using [Line 9](#), i.e., the single proposal weights. For LAIS-dm, in the first iteration the IS weights are computed in [Line 9](#), and in iterations  $J \geq 2$  they are updated in [Line 11](#), which follows from [\(3.17\)](#). This reuses the previously

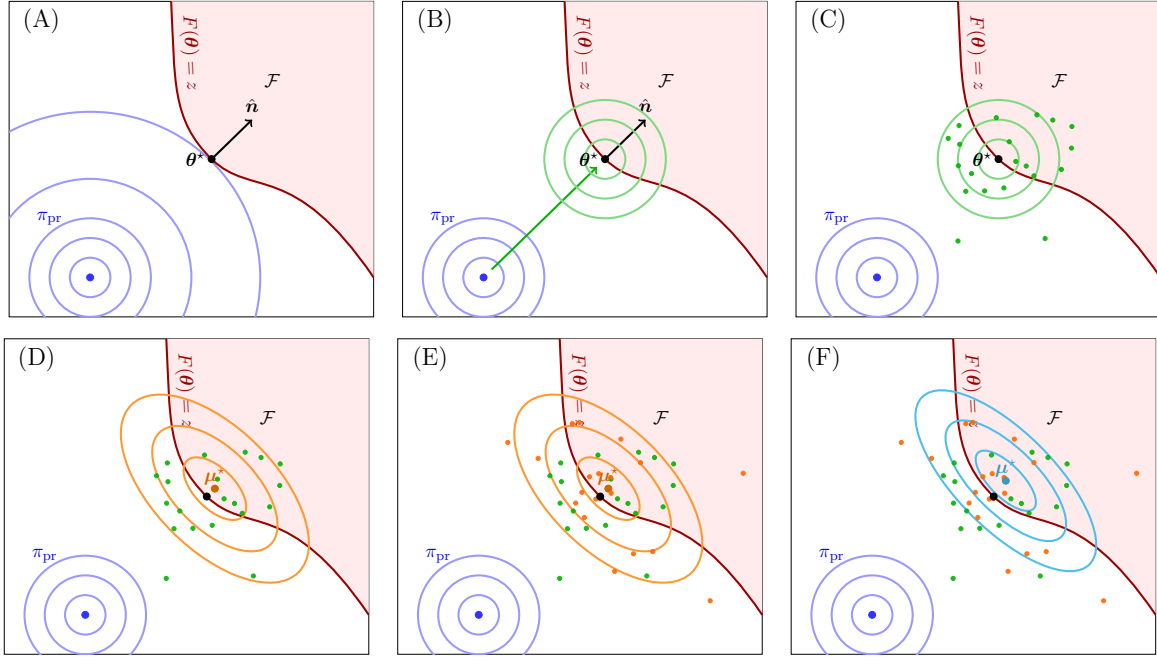


**Figure 1.** Illustration of LAIS: (A) Solve LDT optimization problem (3.1) for  $\theta^*$ , and construct low-dimensional subspace based on local Hessian information; (B) Adaptive importance sampling: start with LSIS (green level sets); (C) AIS: Generate samples from LSIS (green dots); (D) AIS: Use CE to find Gaussian mean and covariance  $\mu^*$  and  $\Sigma^*$  (contour lines in orange); (E) Generate new samples from  $\mathcal{N}(\mu^*, \Sigma^*)$  (orange dots); (F) Use MIS and CE to update  $\mu^*$  and  $\Sigma^*$ , reusing previous samples (orange and green dots) and evaluations.

computed weights  $\{w_i^{(j)}\}_{j=1}^{J-1}$ . Only the IS weights corresponding to  $w_{\text{GIS}}$  (defined in (2.1)) need to be recomputed. In Line 13, we combine subspace samples from the CE-based parametric distribution with samples from the prior in the orthogonal space. To avoid construction of the basis  $\Phi_{\perp}$  of the possibly high-dimensional space orthogonal to  $\Phi_r$ , we first draw samples  $\{\theta_i^{(J)}\}_{i=1}^{N_{\text{CE}}}$  from the original prior distribution  $\pi_{\text{pr}}$ . Then we replace the component in the low-dimensional subspace spanned by  $\Phi_r$  with  $\Phi_r \tilde{\theta}_{r,i}^{(J)}$ .

Note that Algorithm 3.1 takes as input the number of CE iterations, differently from most other CE methods that use a stopping criterion to adaptively choose the number of iterations. For example, a typical criterion is to use the quantile values to ensure that a good portion of samples falls in  $\mathcal{F}$  [10, 32]. Another criterion terminates the iterations when the coefficient of variation of the estimator is smaller than a given threshold [32, 42]. These stopping criteria are usually implemented in the context of intermediate optimal biasing densities, such as adaptively shrinking failure sets [10, 32] or adaptively smoothed indicator functions [32, 42]. Similar stopping criteria can be used in LAIS, but additional work is required to fully justify their applicability. Since the proposed LAIS algorithm does not use intermediate optimal biasing densities, using stopping rules such as quantiles would require extra computations, which are not used in other steps of LAIS. As mentioned in [32], the coefficient of variation of the estimator might not be sufficiently robust when used as stopping criterion. Thus the

**Algorithm 3.1** LDT-based adaptive importance sampling (LAIS)

- 
- 1: **Input:** Function  $F(\boldsymbol{\theta})$ , # of samples per CE step  $N_{\text{CE}}$ , max CE iter.  $J_{\text{max}}$ , threshold  $\epsilon > 0$ .
  - 2: Compute LDT optimizer  $\boldsymbol{\theta}^*$  by solving (3.1)
  - 3: Choose subspace rank  $r$  using  $\epsilon$  as in (3.10) and compute orthonormal basis  $\Phi_r$  as in subsection 3.2.2
  - 4: Set level counter  $J \leftarrow 1$ , total # of samples  $N \leftarrow 0$
  - 5: Set initial mean  $\boldsymbol{\mu}_r^{(1)} = \Phi_r^\top \boldsymbol{\theta}^*$  and covariance  $\boldsymbol{\Sigma}_r^{(1)} = \mathbf{I}_r$
  - 6: **while** True **do**
  - 7: Draw  $N_{\text{CE}}$  samples  $\{\tilde{\boldsymbol{\theta}}_{r,i}^{(j)}\}_{i=1}^{N_{\text{CE}}} \stackrel{\text{i.i.d.}}{\sim} \mathcal{N}(\boldsymbol{\mu}_r^{(j)}, \boldsymbol{\Sigma}_r^{(j)})$
  - 8: **if** s-MIS weights, or  $J = 1$  **then**
  - 9:     Compute weights  $w_i^{(j)} \leftarrow w_{\text{GIS}}(\tilde{\boldsymbol{\theta}}_{r,i}^{(j)}; \boldsymbol{\mu}_r^{(j)}, \boldsymbol{\Sigma}_r^{(j)})$
  - 10: **else**
  - 11:     Update weights:  $w_i^{(j)} \leftarrow (N + N_{\text{CE}}) \left/ \left( \frac{N}{w_i^{(j)}} + \frac{N_{\text{CE}}}{w_{\text{GIS}}(\tilde{\boldsymbol{\theta}}_{r,i}^{(j)}; \boldsymbol{\mu}_r^{(j)}, \boldsymbol{\Sigma}_r^{(j)})} \right) \right.$ ,  $1 \leq j \leq J - 1$  and  
       compute weights for new samples:  $w_i^{(j)} \leftarrow (N + N_{\text{CE}}) \left/ \sum_{j=1}^J \frac{N_{\text{CE}}}{w_{\text{GIS}}(\tilde{\boldsymbol{\theta}}_{r,i}^{(j)}; \boldsymbol{\mu}_r^{(j)}, \boldsymbol{\Sigma}_r^{(j)})} \right.$
  - 12: **end if**
  - 13: Draw  $N_{\text{CE}}$  samples  $\{\boldsymbol{\theta}_i^{(j)}\}_{i=1}^{N_{\text{CE}}} \stackrel{\text{i.i.d.}}{\sim} \pi_{\text{pr}}$  and adjust in low-dim. subspace  $\boldsymbol{\theta}_i^{(j)} \leftarrow \boldsymbol{\theta}_i^{(j)} - \Phi_r \Phi_r^\top \boldsymbol{\theta}_i^{(j)} + \Phi_r \tilde{\boldsymbol{\theta}}_{r,i}^{(j)}$
  - 14: Evaluate  $d_i^{(j)} \leftarrow \mathbb{1}_{\mathcal{F}}(\boldsymbol{\theta}_i^{(j)})$
  - 15: Update  $N \leftarrow N + N_{\text{CE}}$  and compute IS estimator  $\hat{p}_{\mathcal{F}}^{\text{LAIS}} \leftarrow \frac{1}{N} \sum_{j=1}^J \sum_{i=1}^{N_{\text{CE}}} d_i^{(j)} w_i^{(j)}$
  - 16: **if**  $J \geq J_{\text{max}}$  **then**
  - 17:     Break
  - 18: **end if**
  - 19: Compute updated CE mean and covariance
 
$$\boldsymbol{\mu}_r^{(J+1)} := \frac{\sum_{j=1}^J \sum_{i=1}^{N_{\text{CE}}} d_i^{(j)} w_i^{(j)} \tilde{\boldsymbol{\theta}}_{r,i}^{(j)}}{\sum_{j=1}^J \sum_{i=1}^{N_{\text{CE}}} d_i^{(j)} w_i^{(j)}}, \quad \boldsymbol{\Sigma}_r^{(J+1)} := \frac{\sum_{j=1}^J \sum_{i=1}^{N_{\text{CE}}} d_i^{(j)} w_i^{(j)} (\tilde{\boldsymbol{\theta}}_{r,i}^{(j)} - \boldsymbol{\mu}_r^{(J+1)}) (\tilde{\boldsymbol{\theta}}_{r,i}^{(j)} - \boldsymbol{\mu}_r^{(J+1)})^\top}{\sum_{j=1}^J \sum_{i=1}^{N_{\text{CE}}} d_i^{(j)} w_i^{(j)}}$$
  - 20:      $J \leftarrow J + 1$
  - 21: **end while**
  - 22: **Output:**  $\hat{p}_{\mathcal{F}}^{\text{LAIS}}$
- 

authors propose to use the CV of the ratio between the indicator function and its smooth approximation instead. However, this strategy is not applicable for our algorithm since we do not use smoothed indicator functions as intermediate densities. Another concern for adaptively choosing the number of CE iterations based on the quantile or CV is that stopping rules can introduce bias to the estimation, and it is hard to accurately estimate the CV when samples may not be independent. Thus, we use fixed numbers of CE steps in the algorithm to avoid additional computations and bias, and to increase the robustness of the method. Designing an adaptive stopping rule for LAIS that overcomes these challenges would be an interesting

topic for future research.

In [42], a refinement step (Algorithm 2 of [42]) is added to iCERed to further increase accuracy. The basic idea is that the algorithm stops updating the reference parameter, but continues sampling from the current biasing density to evaluate the estimator, until reaching a desired accuracy. A similar approach can also be used in LAIS.

**4. Numerical experiments.** In this section, we compare the performance of the proposed LAIS variants (LAIS-s using standard weights (3.16) and LAIS-dm using deterministic mixture weights (3.17) to compute the MIS estimator) with the iCERed method [42, Algorithm I]. For reference, we also include comparisons with LSIS, which uses the shift provided by the LDT optimizer and can thus be seen as a crude version of LAIS. We use three example problems with increasing difficulties. The first example is quadratic, and thus the LDT optimizer and the eigenvectors and eigenvalues of  $\mathbf{H}_{\text{LDT}}$  are available analytically. The other two examples involve the solution of differential equations. For these examples, we use an adjoint methods to compute gradients, and an interior-point method implemented in the `fmincon` function in MATLAB to solve the optimization problem (3.1). The dominating eigenvectors of the matrix  $\mathbf{H}_{\text{LDT}}$  are computed using MATLAB's `eigs` function. This function only requires the application of  $\mathbf{H}_{\text{LDT}}$  to vectors, which we approximate using finite differences of gradients  $\nabla F$ . For iCERed, the subspace is determined from  $\mathbf{H}_{\text{FIS}}$ , which requires the gradient of the logarithm of the smooth approximation of  $\mathbb{1}_{\mathcal{F}}(\boldsymbol{\theta})$ . We use the smooth approximation  $f(\boldsymbol{\theta}; s)$  defined in (3.7).

**4.1. Quadratic parameter-to-event map  $F$  from [42].** We first consider a quadratic function  $F$ , which is the sum of a linear term and a term that is quadratic in the first two components,

$$(4.1) \quad F(\boldsymbol{\theta}) := \frac{1}{\sqrt{n}} \sum_{k=1}^n \theta_k - \frac{\kappa}{4} (\theta_1 - \theta_2)^2, \quad \boldsymbol{\theta} = [\theta_1, \dots, \theta_n].$$

Since  $F$  is nonlinear only in the first two components, the probability  $p_{\mathcal{F}}$  is independent of the dimension  $n$ . The remaining components result in a half-space and do not effect the measure of the rare event set. The first- and second-order derivatives of  $F$  are:

$$\begin{aligned} \nabla F(\boldsymbol{\theta}) &= \left[ \frac{\kappa}{2}(\theta_2 - \theta_1) + \frac{1}{\sqrt{n}}, \frac{\kappa}{2}(\theta_1 - \theta_2) + \frac{1}{\sqrt{n}}, \frac{1}{\sqrt{n}} \mathbf{1}_{n-2} \right]^{\top}, \\ \nabla^2 F(\boldsymbol{\theta}) &= \begin{bmatrix} -\frac{\kappa}{2} & \frac{\kappa}{2} & & \\ \frac{\kappa}{2} & -\frac{\kappa}{2} & & \\ & & & \mathbf{0}_{n-2} \end{bmatrix}, \end{aligned}$$

where  $\mathbf{0}_{n-2}$  and  $\mathbf{1}_{n-2}$  denote vectors in  $\mathbb{R}^{n-2}$  consisting only of zeros and ones. The LDT optimization (3.1) is a quadratic programming problem with analytic solution  $\boldsymbol{\theta}^* = \frac{z}{\sqrt{n}} \mathbf{1}_n$  and normal direction  $\hat{\mathbf{n}} = \frac{1}{\sqrt{n}} \mathbf{1}_n$ . The Hessian  $\nabla^2 F(\boldsymbol{\theta})$  has rank one, and the eigenvector corresponding to its nonzero eigenvalue is  $\mathbf{y} = [-\frac{\sqrt{2}}{2}, \frac{\sqrt{2}}{2}, 0, \dots, 0]^{\top}$ . Thus, the LDT-informed subspace is spanned by  $\{\hat{\mathbf{n}}, \mathbf{y}\}$  and its dimension is  $r = 2$  (independent of the choices of the threshold  $\epsilon$ ). In all our experiments, the curvature parameter is chosen as  $\kappa = 5$ . The

coefficients of variation shown in this example are based on an average of 100 independent runs for each method.

In [Figure 2](#), we first study the performance of LAIS-s and LAIS-dm in dimensions  $n \in \{2, 334, 1000\}$ . We use different values for the threshold, namely  $z \in \{1, 2, 3, 4, 5, 6\}$ , and compare the relative root-mean-square error (RRMSE,  $\widehat{\text{RRMSE}} := \sqrt{\mathbb{E}[(\hat{p}_{\mathcal{F}} - p_{\mathcal{F}})^2]}/p_{\mathcal{F}}$ ) after  $J_{\max} = 5$  CE updates. Note that the RRMSE requires knowledge of the exact probability  $p_{\mathcal{F}}$ , which is in general not available but can here be computed accurately using numerical integration. Since a different number of samples  $N_{\text{CE}}$  is used in each CE step, the overall number of samples differs for different  $N_{\text{CE}}$ . We observe a similar behavior for the different dimensions, which is a consequence of using  $r = 2$  independently of the dimension  $n$  and the fact that the nonlinearity of  $F$  is restricted to a two-dimensional subspace. Most of the RRMSE for fixed  $N_{\text{CE}}$  (LAIS-s with  $N_{\text{CE}} \geq 200$  and LAIS-dm with all choices of  $N_{\text{CE}}$ ) are insensitive to the target probability, which changes over 10 orders of magnitude. When increasing the number of samples per CE step, the RRMSE decreases, consistent with the expected Monte Carlo convergence rate, as  $O(1/\sqrt{N})$  (note that since the total number of CE steps is fixed,  $O(1/\sqrt{N}) = O(1/\sqrt{N_{\text{CE}}})$ ). In addition, LAIS-dm is insensitive to the dimension and target probability and has smaller absolute errors. In particular, we do not observe bias due to the use of deterministic mixture weights.

Next, in [Figure 3](#), we compare the performance of different methods by plotting their estimated coefficient of variation (CV) and relative root-mean-square error (RRMSE) against the total number  $N$  of samples. This number is a measure for the overall computational cost as we assume sample evaluations to be the dominating operation. We compare both CV and RRMSE because LAIS-dm might have a bias, which would be visible in the RRMSE. We fix  $z = 4$ , resulting in a dimension-independent target probability of  $p_{\mathcal{F}} \approx 6.62 \times 10^{-6}$ . For iCEred, we perform multiple experiments with different parameters and decided to choose  $\varepsilon = 0.01$  and  $\delta = 1.5$  as in [\[42\]](#). We compare LAIS (LAIS-s and LAIS-dm), LSIS and iCEred for different total numbers of samples in different dimensions  $n \in \{2, 334, 1000\}$ . The behavior of all methods is insensitive to the dimensions  $n$  of the random parameter, and RRMSE and CV are almost the same, demonstrating that the bias in LAIS-dm is neglectable. Notice that LAIS results in a much smaller CV and RRMSE compared with LSIS ( $\widehat{\text{CV}}^{\text{LSIS}} \approx 4 \times \widehat{\text{CV}}^{\text{LAIS-DM}}$ ,  $\widehat{\text{CV}}^{\text{LSIS}} \approx 1.5 \times \widehat{\text{CV}}^{\text{LAIS-s}}$ , similar for  $\widehat{\text{RRMSE}}$ ). This is because the proposal used by LSIS is centered at the boundary of the rare event set  $\mathcal{F}$ , which in this problem is strictly convex in the first two components. Thus, substantially more than half of the samples fall outside the rare event set, where  $\mathbb{1}_{\mathcal{F}}$  evaluates to zero. Since LAIS adjusts the mean and covariance of the Gaussian proposal, the result is better tailored to the rare event set. For the same number of total samples, the CV and RRMSE for iCEred are similar to LSIS. Hence, LAIS-dm and LAIS-s outperform iCEred by factors of about 4 and 1.5 in the errors. This is likely since LAIS starts from a good proposal and reuses samples while adaptively refining the mean and covariance. Thus the LAIS estimators uses the total  $N$  evaluations while the iCEred estimator only uses the last  $N_{\text{CE}}$  evaluations.

In [Figure 4](#), we compare the computational cost (total number of samples  $N$ ) for different methods to achieve a fixed RRMSE. The figure is generated by varying different  $N_{\text{CE}}$  and the corresponding total number of iterations, using the same parameter as for the experiments in [Figure 3](#). The computational costs of LSIS and iCEred are similar, and both methods are

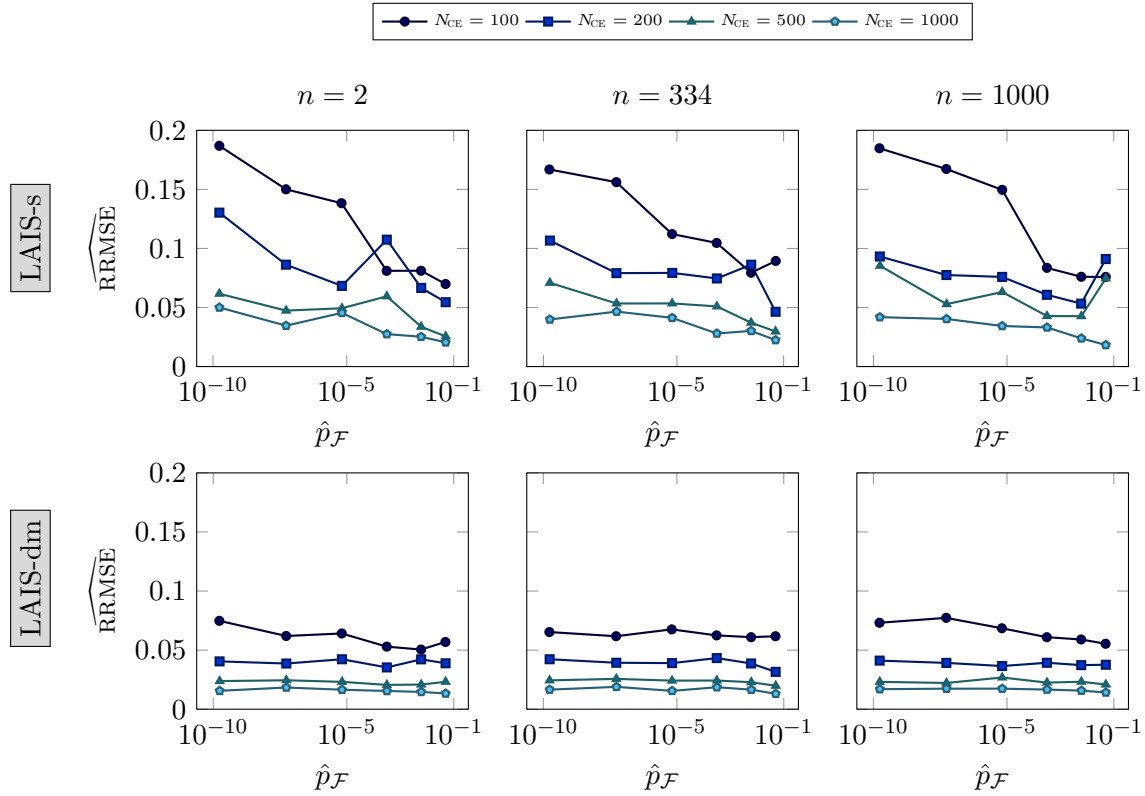


**Figure 2.** Relative root-mean-square error of the rare event probability estimate for the quadratic example (4.1) using different target probabilities. The number of CE updates in Algorithm 3.1 is  $J_{\max} = 5$ . The first row uses standard MIS weights, the second row deterministic mixture MIS weights.

outperformed by the LAIS methods. All methods depend weakly on the extremeness of the events, i.e., the required sample size increases as the target probability decreases. However, the required sample size for LAIS-s and LAIS-dm is more robust to extremeness. For LAIS-dm, the total number of required samples remains mostly constant, demonstrating that LAIS becomes even more advantageous for rarer events.

A possible concern when using tailored Gaussians as biasing densities is a possible degeneration for large  $z$ , since, as predicted by LDT, we expect that the optimal variance in the direction  $\hat{\mathbf{n}}$  decays faster than in the orthogonal directions as  $z$  increases. To study if this is a problem in practice, we calculate the means and covariances of optimal Gaussian distributions for  $z \in \{2, 4, 6\}$  through numerical integration of their analytic form. In Figure 5, we show the resulting 40% and 70% confidence regions in the reduced subspace spanned by normal and tangential directions  $\hat{\mathbf{n}}$  and  $\mathbf{y}$ , respectively. For  $\kappa = 5$  (top of Figure 5), the confidence region of the optimal Gaussian distributions is reduced in all directions as  $z \rightarrow \infty$ . As expected, it decays slightly faster in the normal direction. However, we do not observe a degeneration as the ratio only varies moderately over a wide range of probabilities<sup>1</sup> The results for  $\kappa = -0.1$

<sup>1</sup>For  $z = 6$ , the probability  $p_{\mathcal{F}}$  is around  $10^{-10}$ .

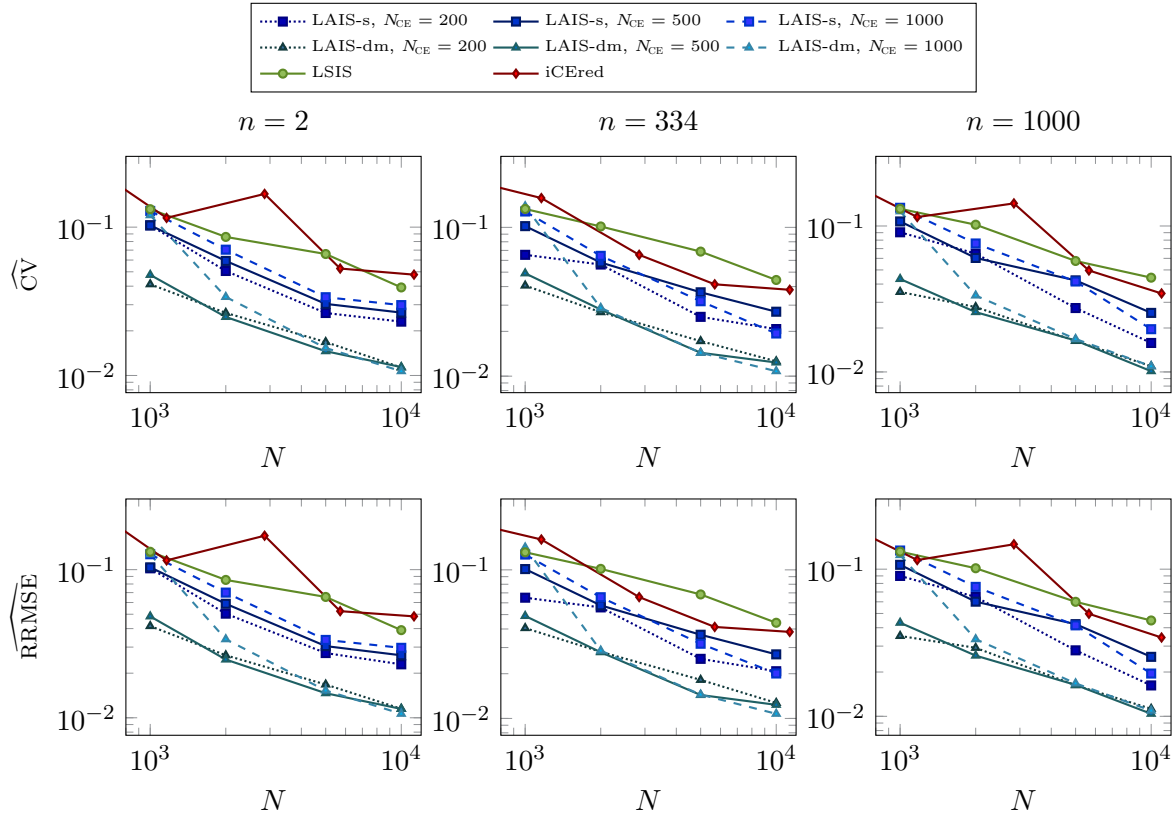


**Figure 3.** Comparison of coefficient of variation and relative root-mean-square error versus overall number  $N$  of sample evaluations for quadratic example (4.1). Shown is the behavior of different methods for fixed threshold  $z = 4$ .

are shown at the bottom of Figure 5. Here, for growing  $z$ , the confidence region increases in the  $\mathbf{y}$ -direction while it decreases in the normal direction  $\hat{\mathbf{n}}$ . The optimal Gaussian becomes “slim”, but the ratio is still reasonable and unlikely to lead to numerical problems. This suggests that degeneration of approximating Gaussians and potentially resulting numerical instabilities does not seem to be a substantial problem, at least for this example. If one encounters fast degeneracy of the optimal Gaussian density in the normal direction, then special treatments in that direction may be required. For example, one could use an exponential density function in the normal direction. However, in that case, an explicit formula similar to (2.8) would not be available since the parametrized distribution would not be Gaussian; see also the discussion in section 5.

Finally, due to the simplicity of (4.1), analytic expressions of the LDT optimizer and the LDT-informed subspace are available. In general, solving the LDT optimization problem as well as finding the LDT-informed subspace require numerical computations. These increase the computational cost of LAIS. Also iCERed requires additional evaluations of gradients of  $F$  to find the low-rank subspaces. When the evaluation of  $F$  is complicated, e.g., when it

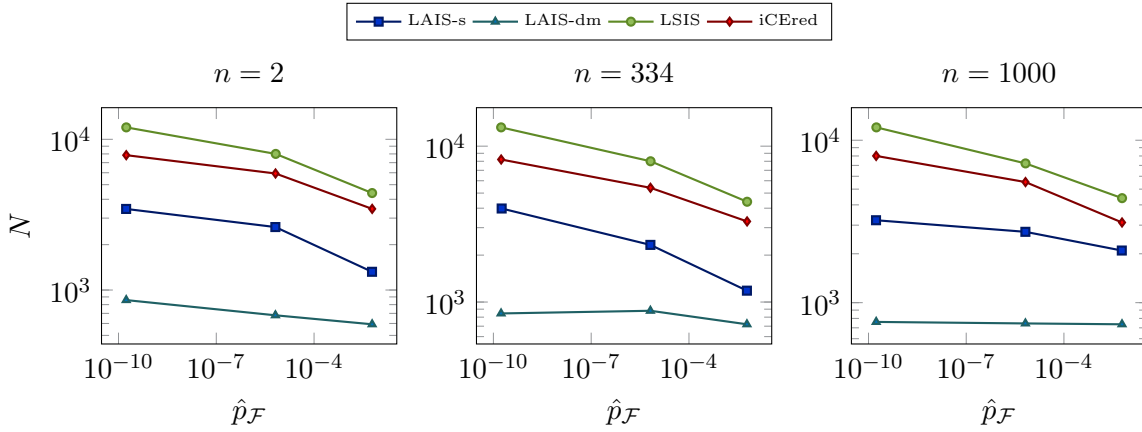


**Figure 4.** Comparison of number of totally required samples  $N$  for different methods to obtain an RRMSE in the range  $[4.5 \times 10^{-2}, 5 \times 10^{-2}]$  using different target probabilities  $\hat{p}_{\mathcal{F}}$  and problem dimensions  $n$ .

involves the solution of a differential equation, the evaluation of  $F$  and its gradients typically dominate the overall computational cost. The next two problems are examples where this is the case.

**4.2. 1D diffusion problem from [45].** Next, we consider a 1D diffusion problem defined on the domain  $D = [0, 1]$ . The stochastic differential equation is

$$(4.2) \quad \begin{aligned} -\frac{\partial}{\partial x} \left( a(x, \omega) \frac{\partial}{\partial x} v(x, \omega) \right) &= 1, \quad x \in [0, 1], \\ v(0, \omega) &= 0, \\ v'(1, \omega) &= 0, \end{aligned}$$

for almost every  $\omega \in \Omega$ . The coefficient function  $a(x, \omega)$  is a log-normal random field with mean  $\mathbb{E}[a(x, \cdot)] = 1$  and  $\mathbb{V}[a(x, \cdot)] = 0.01$ . Assuming that  $a(x, \omega) = \exp(Z(x, \omega))$ , then  $Z(x, \omega)$  is a Gaussian random field with mean  $\mu_Z = \ln(\mathbb{E}[a(x, \cdot)]) - \sigma_Z^2/2$  and variance  $\sigma_Z^2 = \ln((\mathbb{V}[a(x, \cdot)] + \mathbb{E}[a(x, \cdot)]^2)/\mathbb{E}[a(x, \cdot)]^2)$ . The covariance operator is defined as  $c(x, y) = \sigma_Z^2 \exp(-|x - y|/l)$  with correlation length  $l = 0.01$ . The truncated KL expansion of  $Z(x, \omega)$  is

$$(4.3) \quad Z(x, \omega) = \mu_Z + \sum_{m=1}^n \sqrt{\lambda_m} e_m(x) \theta_m(\omega),$$

where  $(\lambda_m, e_m)$  are eigenpairs of  $c(x, y)$ , and we use the dimension  $n = 150$ . The random parameter  $\boldsymbol{\theta} \in \mathbb{R}^n$  and  $\boldsymbol{\theta} \sim \mathcal{N}(\mathbf{0}, \mathbf{I}_n)$ . The eigenpairs of  $c(x, y)$  are obtained using the Nystrom method [33] with one Gauss-Legendre point in each element (512 equidistant elements in total).

The event we are interested in is the value of the state at the endpoint  $x = 1$ , and we use the threshold  $z = 0.535$ , i.e., we are interested in the probability that

$$(4.4) \quad F(\boldsymbol{\theta}) := v(1, \omega) \geq 0.535.$$

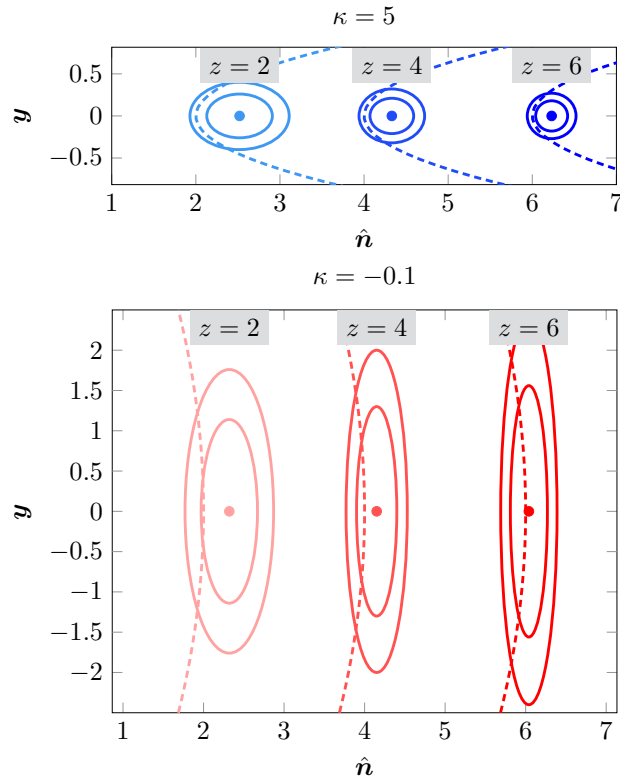


**Figure 5.** Comparison of mean and confidence regions of optimal Gaussian biasing distributions in the two-dimensional reduced subspace for the quadratic problem (4.1) and for different  $z$ . The top figure is for  $\kappa = 5$  and the bottom one for  $\kappa = -0.1$ . The x-axis corresponds to the normal direction  $\hat{n}$ , and the y-axis to direction  $\mathbf{y}$ , the only non-zero curvature direction. The dots are the optimal means  $\boldsymbol{\mu}^*$ , and the ellipses show the 40% and 70% confidence regions. The dashed lines are the boundaries of the rare event sets, which are to the right to the boundary.

The corresponding rare event probability is  $p_{\mathcal{F}} \approx 1.63 \times 10^{-4}$  (computed using LSIS with  $5 \times 10^6$  samples). We use a finite element method with 512 elements and linear basis functions to discretize (4.2). The adjoint method is used to obtain the gradient  $\nabla F(\boldsymbol{\theta})$ .

In Figure 6, we compare LAIS (LAIS-s and LAIS-dm), iCEred and LSIS with respect to the required total number of evaluations of  $F$  (denoted as  $N_F$ ). The results are from an average of 100 independent runs of each method. The rank  $r$  for LAIS is chosen based on the absolute values of eigenvalues of  $\mathbf{H}_{\text{LDT}}$ . For the different algorithms, we estimate the RRMSE and CV, which are again similar. The only difference occurs for LAIS-dm with  $N_{\text{CE}} = 500, r = 5$  when  $N_F \leq 2 \times 10^3$ , which is mainly due to the dependency between samples being stronger for the first iterations ( $J \leq 4$ ) when the dimension of reference parameter  $O(r^2)$  is large and the sample size  $N_{\text{CE}}$  is small. These discrepancies disappear after several iterations. Thus, the potential bias in LAIS-dm is controllable.

In general, the LDT-informed methods LSIS and LAIS outperform iCEred. LSIS and iCEred perform more similarly as the total number of samples increases, but LSIS still outperforms iCEred by a factor of 1.5 in terms of errors. The RRMSE and CV of LAIS-dm are

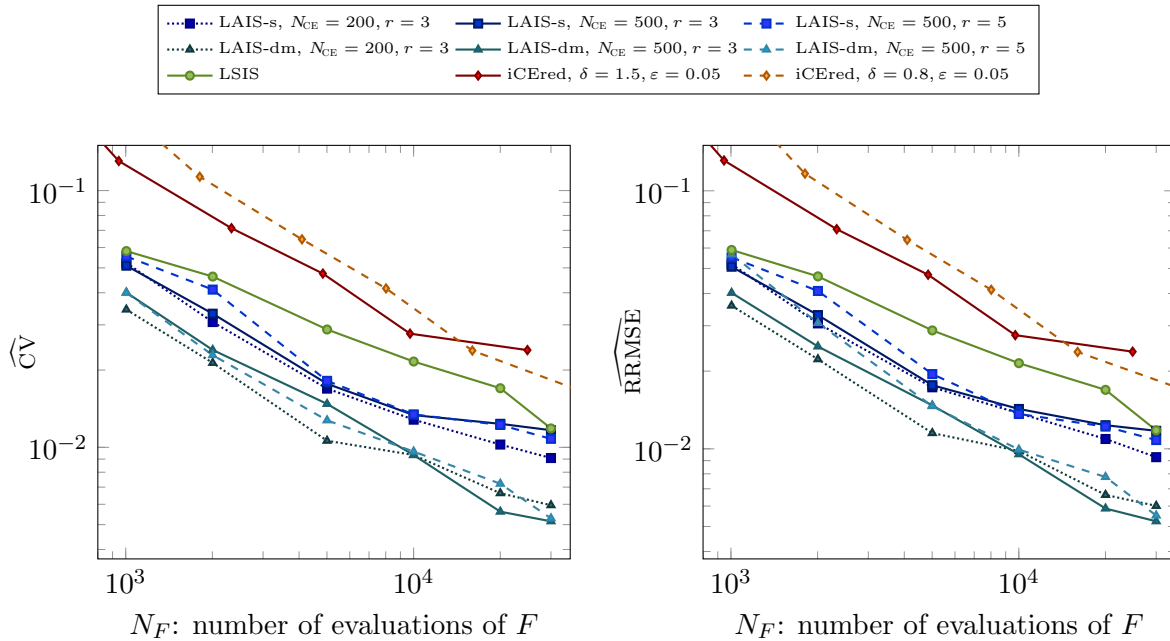


**Figure 6.** Comparison of coefficient of variation and relative root-mean-square error plotted against number  $N_F$  of evaluations of  $F$  for 1D diffusion problem. Shown are results obtained with LAIS, LSIS and iCEred with various parameter choices.

more than 3 times smaller than iCEred (2.5 times smaller than LSIS), those of LAIS-s are more than 2 times smaller than iCEred (1.5 times smaller than LSIS).

To study the robustness of the algorithms, we vary the number of samples per CE step  $N_{\text{CE}} = \{200, 500\}$  and the rank  $r = \{3, 5\}$  used for the subspace in LAIS. The latter ranks correspond to the thresholds  $\epsilon = 0.075$  for  $r = 3$  and  $\epsilon = 0.065$  for  $r = 5$  in (3.10). In iCEred, we use different  $\delta = \{0.8, 1.5\}$ , and  $\epsilon = 0.05$ . We choose  $N_{\text{CE}}$  in iCEred such that we obtain different total numbers of evaluations of  $F$ . The average number of levels for iCEred is 4, and the final rank depends on  $N_{\text{CE}}$ , with an average:  $r = 6$  for  $N_{\text{CE}} = 200$  and  $r = 12$  for  $N_{\text{CE}} = 500$ , which is slightly larger than the ones we use for LAIS. LAIS with different ranks of the subspace and different  $N_{\text{CE}}$  per CE steps perform similarly, demonstrating that the algorithm is rather insensitive to these choices. We find the performance of iCEred depends on  $\delta$ , which controls the decay of the smoothing parameter  $s$  from level to level, and at what point the method terminates.

Note that in Figure 6, we only report  $N_F$ , the number of evaluations of  $F$ . For LAIS and LSIS, this number is  $N_F = N + 5$ , where  $N$  is the total number of samples, and the extra five evaluations come from solving the constrained optimization. For iCEred, this number is the same as the total number of samples  $N_F = N$ . However, there is a large difference in the number of gradient evaluations (we denote this number by  $N_{\nabla F}$ ) in LAIS, LSIS and iCEred. For LAIS and LSIS, the optimization step requires 4 gradient computations, while the eigenvalue estimation requires 50-60 gradients, thus the total number of gradient computations

is  $N_{\nabla F} \leq 70$ , largely independent of  $r$  and  $N_{\text{CE}}$ . The iCERed method does not require solution of an optimization problem, but constructs the matrix (3.4) for every level, which requires evaluation of  $\nabla F$  for each evaluation of  $F$ . Thus, the number of gradient evaluations for iCERed is  $N_{\nabla F} = N$ . Since we use an adjoint method to compute gradients, one gradient evaluation amounts to solving an additional boundary value problem (the adjoint equation). Thus, the total cost (ODE/PDE solves) for iCERed is  $N_F + N_{\nabla F} \approx 2N$ , while the number for LAIS and LSIS remains approximately  $N$ .

**4.3. Tsunami problem.** Finally, we consider a more realistic problem, where we estimate the probability of the extreme tsunami wave height on shore. This example is adapted from Section 5 in [40]. To model tsunami waves, we use the one-dimensional shallow water equations [26] defined on a domain  $\mathcal{D} = [a, b]$  for times  $t \in [0, T_F]$ . The domain represents a slice through the sea, that includes the shallow part near the shore and the part where the ocean floor elevation can change unpredictably during an earthquake. We denote the horizontal fluid velocity as  $u(x, t)$  and the height of water above the ocean floor by  $h(x, t)$ . The bathymetry  $B(x)$  is the negative depth of the ocean, i.e.,  $h(x, t) + B(x) = 0$  when the ocean is at rest. Introducing the variable  $v := hu$ , the shallow water equations can be written as

$$(4.5a) \quad h_t + v_x = 0 \quad \text{on } \mathcal{D} \times [0, T_F],$$

$$(4.5b) \quad v_t + \left( \frac{v^2}{h} + \frac{1}{2}gh^2 \right)_x + ghB_x = 0 \quad \text{on } \mathcal{D} \times [0, T_F],$$

$$(4.5c) \quad h(x, 0) = -B_0(x), \quad v(x, 0) = 0 \quad \text{for } x \in \mathcal{D},$$

$$(4.5d) \quad v(a, t) = v(b, t) = 0 \quad \text{for } t \in [0, T_F],$$

where  $g$  is the gravitational constant and the subscripts  $t, x$  denote derivatives with respect to time and location.  $B_0(x)$  is the reference bathymetry before any changes and is chosen based on the real topography [17, 40].

The bathymetry  $B(x)$ , whose derivative enters in the right hand side of (4.5), changes during an earthquake as a result of slip between plates under the ocean floor. Since details of this slip process are difficult to predict, we model the slip as a random process, and thus also the bathymetry field  $B$  is random. Since  $B$  enters in the shallow water equations (4.5), the (space and time-dependent) solutions  $h$  and  $v$  are random and hence also the event objective we specify below is a random variable. Random bathymetry changes are caused by slips under the earth between two plates, which we propagate to the ocean floor using the Okada model [29]. Thus, we can denote the random parameter  $\boldsymbol{\theta}$  in this problem as these slips, with relation

$$(4.6) \quad B(x) = B_0(x) + \sigma(O\boldsymbol{\theta})(x) \quad \text{with } \boldsymbol{\theta} = (\theta_1, \dots, \theta_{20})^\top \quad \text{and } (O\boldsymbol{\theta})(x) := \sum_{i=1}^{20} \theta_i O_i(x),$$

where  $O_i$  is the bathymetry change due to the  $i$ th slip patch,  $\sigma^2 = 10$  and  $\boldsymbol{\theta} \sim \mathcal{N}(\mathbf{0}, \mathbf{I}_{20})$ .

The final observation is a smooth approximation of the maximal average tsunami wave height in the interval  $[c, d]$  on shore over the time period  $[0, T_F]$ , i.e.,

$$(4.7) \quad F(\boldsymbol{\theta}) := \gamma \ln \left[ \frac{1}{T_F} \int_0^{T_F} \exp \left( \frac{1}{\gamma} \int_c^d (h + B_0) dx \right) dt \right],$$

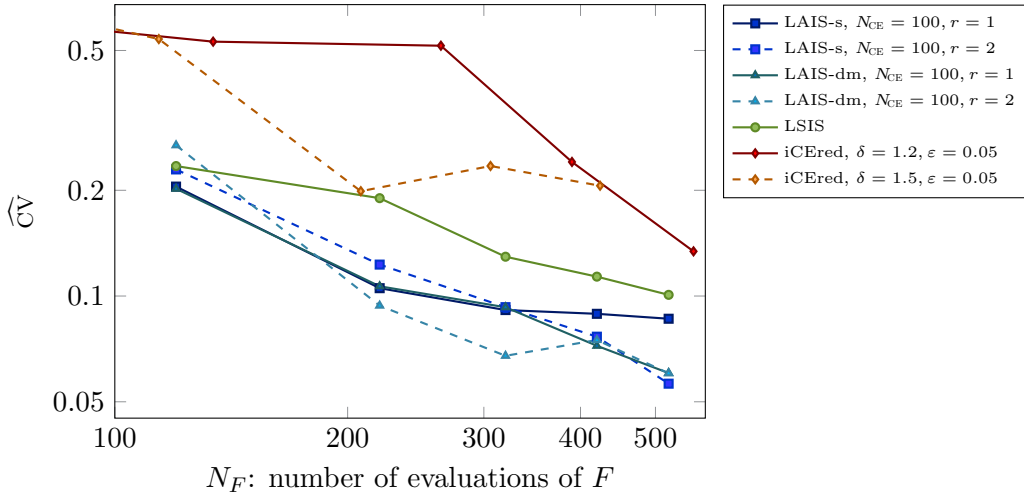


**Figure 7.** Comparison of coefficient of variation for tsunami problem for different algorithms. As before, the comparison is with respect to the necessary number of evaluations of  $F$ , each of which requires the solution of a time-dependent 1D shallow water equation.

where we choose  $\gamma = 0.003$ . The event threshold is  $z = 0.5737$ , i.e., we are interested in estimating the probability that  $F(\theta) \geq 0.5737$ . We compare the coefficient of variation from an average of 10 independent runs of LAIS, LSIS and iCEred for different total number of evaluations of  $F$  in Figure 7 and different subspace ranks  $r = 1$  and  $r = 2$ , which correspond to  $\epsilon = 0.6$  and  $\epsilon = 0.05$ , respectively. We observe that LAIS (both variants with standard and deterministic mixture weights) achieve a lower CV compared to the other two methods, and also performs robustly with respect to the numerical parameters in the algorithm. While more comparisons will be necessary to compare these algorithms rigorously for complex, PDE-governed problems, this indicates the efficiency of LAIS for estimating low probabilities in complex systems.

**5. Conclusion and discussions.** We developed an adaptive importance sampling scheme for rare event probability estimation in high dimensions. The approach (called LAIS) combines ideas from large deviation theory (LDT), importance sampling (IS) based on cross-entropy (CE), and multiple importance sampling (MIS). It consists of: (1) a sampling-free preprocessing step, namely finding the LDT optimizer and using second-order derivative information to identify an intrinsic low-dimensional subspace that is most informative of the rare event probability. Additionally, the LDT optimizer provides a good initial proposal for AIS; (2) an adaptive sampling procedure: using CE to update a Gaussian proposal and MIS to build an estimator that reuses all previous sample evaluations. Our method improves the state-of-the-art iCEred method proposed in [42] in several directions. LAIS achieves a consistently smaller coefficient of variance and relative root-mean-square error compared with iCEred for the same number of evaluations of  $F$ , since all samples in step (2) are used in the final estimator, and since even the initial set of samples are informative as they are guided by the LDT optimizer. LAIS requires no gradient evaluations in step (2) and  $O(10)$  ( $< 70$  in our examples) gradient evaluations in step (1), while iCEred requires gradient computation for each sample. In

addition, LAIS does not require tuning numerical parameters that have significant influence on the performance of the algorithm. A choice one has to make is  $N_{\text{CE}}$ , i.e., how often one updates the biasing density, but as long as  $N_{\text{CE}}$  is moderately large ( $\geq 200$ ), the performance is robust with respect to this choice. Another numerical parameter in LAIS is the rank of the low-dimensional subspace, which is chosen based on the magnitude of eigenvalues of  $\mathbf{H}_{\text{LDT}}$  (see subsection 3.2.2). In our experiments, the performance of LAIS is stable as long as we include the normal direction  $\nabla F(\boldsymbol{\theta}^*)$ .

There are opportunities to refine and extend LAIS. First, a variant of LAIS with deterministic mixture weights that can be proven to be bias-free would be desirable. A potential introduction of bias in adaptive multiple importance samplers is, however, a known challenge [7]. Further, the parametric biasing distributions used in this paper are Gaussians, which may suffer from degeneracy in high-dimensions for problems without intrinsic low-rank structure. Thus, one could explore the use of more general parametric models such as the von Mises-Fisher-Nakagami mixture [32], or a normalizing flow model from machine learning [24]. Another extension is to apply LAIS for infinite-dimensional or non-Gaussian prior distributions. For infinite-dimensional problem with intrinsic low-rank structure, the main difficulty is to properly define the weights and biasing densities. There are several challenges to extend LAIS to non-Gaussian distributions. Firstly, the LDT rate function is no longer quadratic, and needs to be derived or even implicitly used in the form of the Legendre transform of the cumulant generating function (some examples can be found in [39, 40]) when solving the LDT optimization problem (3.1). In addition, both the local LIS and Theorem 3.1 are based on a Gaussian prior, thus the technique of identifying a low-dimensional subspace in LAIS is no longer valid for non-Gaussian distributions. Certified dimension reduction using  $\mathbf{H}_{\text{FIS}}$  [47] may be a possible alternative.

**Acknowledgments.** We appreciate many helpful discussions with Eric Vanden-Eijnden and Timo Schorlepp.

## REFERENCES

- [1] S.-K. AU AND J. L. BECK, *Estimation of small failure probabilities in high dimensions by subset simulation*, Probabilistic Engineering Mechanics, 16 (2001), pp. 263–277.
- [2] J. A. BILMES, *A gentle tutorial of the EM algorithm and its application to parameter estimation for Gaussian mixture and hidden Markov models*, International Computer Science Institute, 4 (1998), p. 126.
- [3] J. BUCKLEW, *Introduction to rare event simulation*, Springer, 2007.
- [4] M. F. BUGALLO, V. ELVIRA, L. MARTINO, D. LUENGO, J. MIGUEZ, AND P. M. DJURIC, *Adaptive importance sampling: The past, the present, and the future*, IEEE Signal Processing Magazine, 34 (2017), pp. 60–79.
- [5] O. CAPPÉ, A. GUILLIN, J.-M. MARIN, AND C. P. ROBERT, *Population Monte Carlo*, Journal of Computational and Graphical Statistics, 13 (2004), pp. 907–929.
- [6] F. CÉROU, P. DEL MORAL, T. FURON, AND A. GUYADER, *Sequential Monte Carlo for rare event estimation*, Statistics and computing, 22 (2012), pp. 795–808.
- [7] J.-M. CORNUET, J.-M. MARIN, A. MIRA, AND C. P. ROBERT, *Adaptive multiple importance sampling*, Scandinavian Journal of Statistics, 39 (2012), pp. 798–812.
- [8] T. CUI, J. MARTIN, Y. M. MARZOUK, A. SOLONEN, AND A. SPANTINI, *Likelihood-informed dimension reduction for nonlinear inverse problems*, Inverse Problems, 30 (2014), p. 114015.

- [9] J. K. CULLUM AND R. A. WILLOUGHBY, *Lanczos Algorithms for Large Symmetric Eigenvalue Computations, Vol. 1: Theory*, Progress in Scientific Computing, Birkhäuser-Verlag, Boston, Basel, Berlin, 1985.
- [10] P.-T. DE BOER, D. P. KROESE, S. MANNOR, AND R. Y. RUBINSTEIN, *A tutorial on the cross-entropy method*, Annals of Operations Research, 134 (2005), pp. 19–67.
- [11] G. DEMATTEIS, T. GRAFKE, AND E. VANDEN-ELJNDEN, *Extreme event quantification in dynamical systems with random components*, SIAM/ASA Journal on Uncertainty Quantification, 7 (2019), pp. 1029–1059.
- [12] A. DEMBO AND O. ZEITOUNI, *Large Deviations Techniques and Applications*, Applications of Mathematics, Springer, 1998.
- [13] O. DITLEVSEN AND H. O. MADSEN, *Structural reliability methods*, vol. 178, Wiley New York, 1996.
- [14] O. DITLEVSEN, R. E. MELCHERS, AND H. GLUVER, *General multi-dimensional probability integration by directional simulation*, Computers & Structures, 36 (1990), pp. 355–368.
- [15] X. DU AND W. CHEN, *A most probable point-based method for efficient uncertainty analysis*, Journal of Design and Manufacturing Automation, 4 (2001), pp. 47–66.
- [16] L. EBENER, G. MARGAZOGLU, J. FRIEDRICH, L. BIFERALE, AND R. GRAUER, *Instanton based importance sampling for rare events in stochastic PDEs*, Chaos: An Interdisciplinary Journal of Nonlinear Science, 29 (2019), p. 063102.
- [17] T. FUJIWARA, S. KODAIRA, T. NO, Y. KAIHO, N. TAKAHASHI, AND Y. KANEDA, *The 2011 Tohoku-Oki earthquake: Displacement reaching the trench axis*, Science, 334 (2011), pp. 1240–1240.
- [18] S. GEYER, I. PAPAIOANNOU, AND D. STRAUB, *Cross entropy-based importance sampling using Gaussian densities revisited*, Structural Safety, 76 (2019), pp. 15–27.
- [19] T. GRAFKE AND E. VANDEN-ELJNDEN, *Numerical computation of rare events via large deviation theory*, Chaos: An Interdisciplinary Journal of Nonlinear Science, 29 (2019), p. 063118.
- [20] N. HALKO, P. G. MARTINSSON, AND J. A. TROPP, *Finding structure with randomness: Probabilistic algorithms for constructing approximate matrix decompositions*, SIAM Review, 53 (2011), pp. 217–288.
- [21] T. HESTERBERG, *Weighted average importance sampling and defensive mixture distributions*, Technometrics, 37 (1995), pp. 185–194.
- [22] H. KAHN AND A. W. MARSHALL, *Methods of reducing sample size in Monte Carlo computations*, Journal of the Operations Research Society of America, 1 (1953), pp. 263–278.
- [23] L. S. KATAFYGIOTIS AND K. M. ZUEV, *Geometric insight into the challenges of solving high-dimensional reliability problems*, Probabilistic Engineering Mechanics, 23 (2008), pp. 208–218.
- [24] I. KOBYZEV, S. J. PRINCE, AND M. A. BRUBAKER, *Normalizing flows: An introduction and review of current methods*, IEEE transactions on pattern analysis and machine intelligence, 43 (2020), pp. 3964–3979.
- [25] M. LEMAIRE, *Structural reliability*, John Wiley & Sons, 2013.
- [26] R. J. LEVEQUE AND D. L. GEORGE, *High-resolution finite volume methods for the shallow water equations with bathymetry and dry states*, in Advanced numerical models for simulating tsunami waves and runup, World Scientific, 2008, pp. 43–73.
- [27] J. S. LIU, *Monte Carlo strategies in scientific computing*, Springer Science & Business Media, 2008.
- [28] N. METROPOLIS AND S. ULAM, *The Monte Carlo method*, Journal of the American statistical association, 44 (1949), pp. 335–341.
- [29] Y. OKADA, *Surface deformation due to shear and tensile faults in a half-space*, Bulletin of the seismological society of America, 75 (1985), pp. 1135–1154.
- [30] A. OWEN AND Y. ZHOU, *Safe and effective importance sampling*, Journal of the American Statistical Association, 95 (2000), pp. 135–143.
- [31] T. PAANANEN, J. PIIRONEN, P.-C. BÜRKNER, AND A. VEHTARI, *Implicitly adaptive importance sampling*, Statistics and Computing, 31 (2021), pp. 1–19.
- [32] I. PAPAIOANNOU, S. GEYER, AND D. STRAUB, *Improved cross entropy-based importance sampling with a flexible mixture model*, Reliability Engineering & System Safety, 191 (2019), p. 106564.
- [33] W. H. PRESS, S. A. TEUKOLSKY, W. T. VETTERLING, AND B. P. FLANNERY, *Numerical recipes 3rd edition: The art of scientific computing*, Cambridge university press, 2007.
- [34] R. RACKWITZ, *Reliability analysis – a review and some perspectives*, Structural Safety, 23 (2001), pp. 365–

- 395.
- [35] R. Y. RUBINSTEIN, *Optimization of computer simulation models with rare events*, European Journal of Operational Research, 99 (1997), pp. 89–112.
  - [36] T. P. SAPSIS, *New perspectives for the prediction and statistical quantification of extreme events in high-dimensional dynamical systems*, Philosophical Transactions of the Royal Society A: Mathematical, Physical and Engineering Sciences, 376 (2018), p. 20170133.
  - [37] T. SCHORLEPP, T. GRAFKE, S. MAY, AND R. GRAUER, *Spontaneous symmetry breaking for extreme vorticity and strain in the three-dimensional Navier–Stokes equations*, Philosophical Transactions of the Royal Society A, 380 (2022), p. 20210051.
  - [38] G. I. SCHÜELLER AND R. STIX, *A critical appraisal of methods to determine failure probabilities*, Structural Safety, 4 (1987), pp. 293–309.
  - [39] S. TONG, A. SUBRAMANYAM, AND V. RAO, *Optimization under rare chance constraints*, SIAM Journal on Optimization, 32 (2022), pp. 930–958.
  - [40] S. TONG, E. VANDEN-EIJNDEN, AND G. STADLER, *Extreme event probability estimation using PDE-constrained optimization and large deviation theory, with application to tsunamis*, Communications in Applied Mathematics and Computational Science, 16 (2021), pp. 181–225.
  - [41] E. ULLMANN AND I. PAPAIOANNOU, *Multilevel estimation of rare events*, SIAM/ASA Journal on Uncertainty Quantification, 3 (2015), pp. 922–953.
  - [42] F. URIBE, I. PAPAIOANNOU, Y. M. MARZOUK, AND D. STRAUB, *Cross-entropy-based importance sampling with failure-informed dimension reduction for rare event simulation*, SIAM/ASA Journal on Uncertainty Quantification, 9 (2021), pp. 818–847.
  - [43] S. R. S. VARADHAN, *Large deviations and applications*, vol. 46, SIAM, 1984.
  - [44] E. VEACH AND L. J. GUIBAS, *Optimally combining sampling techniques for Monte Carlo rendering*, in Proceedings of the 22nd annual conference on Computer graphics and interactive techniques, 1995, pp. 419–428.
  - [45] F. WAGNER, J. LATZ, I. PAPAIOANNOU, AND E. ULLMANN, *Multilevel sequential importance sampling for rare event estimation*, SIAM Journal on Scientific Computing, 42 (2020), pp. A2062–A2087.
  - [46] S. WAHAL AND G. BIROS, *BIMC: The Bayesian inverse Monte Carlo method for goal-oriented uncertainty quantification. Part I*, arXiv preprint arXiv:1911.00619, (2019).
  - [47] O. ZAHM, T. CUI, K. LAW, A. SPANTINI, AND Y. MARZOUK, *Certified dimension reduction in nonlinear Bayesian inverse problems*, Mathematics of Computation, 91 (2022), pp. 1789–1835.